Simulation Models of PCM Storage Units

A Report of IEA Solar Heating and Cooling programme - Task 32

“Advanced storage concepts for solar and low energy buildings”

Report C5 of Subtask C

March 2008

Edited by:
Wolfgang Streicher

Contributions from:
Jacques Bony
Stephane Citherlet
Andreas Heinz
Peter Puschnig
Hermann Schranzhofer
Jørgen M. Schultz

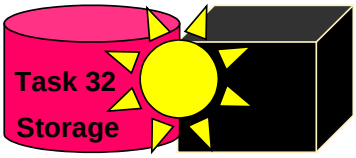

SHC
SOLAR HEATING & COOLING PROGRAMME
INTERNATIONAL ENERGY AGENCY

Project Report C5 of Subtask C

Simulation models of PCM Storage Units

by

Wolfgang Streicher (Editor)*

Project data by:

Bony, J, Citherlet, S., HEIG-VD, Yverdon-les-Bains (Switzerland),
Heinz, A., Puschnig, P., Schranzhofer, H., Institute of Thermal Engineering,
Graz University of Technology (Austria)
Schultz, J., M., Furbo, S., BYG DTU, Department of Civil Engineering (Denmark)

A technical report of Subtask C

IWT TU Graz
Institut für Wärmetechnik

TU Graz
Graz University of Technology

*Institute of Thermal Engineering
Graz University of Technology Austria
Inffeldgasse 25 B, A-8010 Graz
w.streicher@tugraz.at
www.iwt.tugraz.at

Executive Summary

In the course of IEA SHC Task 32 the following simulation models were developed

- Two tank heat storage models with PCM containers of different shapes (plates, cylinders, spheres) with variable size and number (Type 840 and Type 860). Different PCMs can be chosen and the models include the subcooling and the hysteresis behavior of the PCM.
- In the Type 860 of Bony (HEIVG) the internal heat transfer by convection in the liquid PCM is accounted for.
- The tank model of Heinz and Puschnig (IWT, Type 840) can also be filled completely with PCM slurry that can be used as heat carrier
- One model (Type 841) OF Heinz (IWT) with an immersed heat exchanger into a PCM container
- One tank model (Type 185 of Schultz, DTU) for seasonal heat storage with PCM in subcooled state

All models were validated by experiments and are suitable for the TRNSYS simulation environment. Nevertheless the authors do NOT take any responsibility for the results of the models.

All models were used for yearly system simulations including PCM storage.

With these models there is now the opportunity to develop optimized systems with various PCM store, hydraulic and control configurations and to compare PCM heat store systems with water heat store systems.

The use of the models for the public is decided by the author of the model individually.

SOLAR HEATING & COOLING PROGRAMME
INTERNATIONAL ENERGY AGENCY

IEA Solar Heating and Cooling Programme

The *International Energy Agency* (IEA) is an autonomous body within the framework of the Organization for Economic Co-operation and Development (OECD) based in Paris. Established in 1974 after the first "oil shock," the IEA is committed to carrying out a comprehensive program of energy cooperation among its members and the Commission of the European Communities.

The IEA provides a legal framework, through IEA Implementing Agreements such as the *Solar Heating and Cooling Agreement*, for international collaboration in energy technology research and development (R&D) and deployment. This IEA experience has proved that such collaboration contributes significantly to faster technological progress, while reducing costs; to eliminating technological risks and duplication of efforts; and to creating numerous other benefits, such as swifter expansion of the knowledge base and easier harmonization of standards.

The *Solar Heating and Cooling Programme* was one of the first IEA Implementing Agreements to be established. Since 1977, its members have been collaborating to advance active solar and passive solar and their application in buildings and other areas, such as agriculture and industry. Current members are:

Australia	Finland	Portugal
Austria	France	Spain
Belgium	Italy	Sweden
Canada	Mexico	Switzerland
Denmark	Netherlands	United States
European Commission	New Zealand	
Germany	Norway	

A total of 39 Tasks have been initiated, 30 of which have been completed. Each Task is managed by an Operating Agent from one of the participating countries. Overall control of the program rests with an Executive Committee comprised of one representative from each contracting party to the Implementing Agreement. In addition to the Task work, a number of special activities—Memorandum of Understanding with solar thermal trade organizations, statistics collection and analysis, conferences and workshops—have been undertaken.

The Tasks of the IEA Solar Heating and Cooling Programme, both underway and completed are as follows:

Current Tasks:

Task 32 *Advanced Storage Concepts for Solar and Low Energy Buildings*
Task 33 *Solar Heat for Industrial Processes*
Task 34 *Testing and Validation of Building Energy Simulation Tools*
Task 35 *PV/Thermal Solar Systems*
Task 36 *Solar Resource Knowledge Management*
Task 37 *Advanced Housing Renovation with Solar & Conservation*
Task 38 *Solar Assisted Cooling Systems*
Task 39 *Polymeric Materials for Solar Thermal Applications*

Completed Tasks:

Task 1 *Investigation of the Performance of Solar Heating and Cooling Systems*
Task 2 *Coordination of Solar Heating and Cooling R&D*
Task 3 *Performance Testing of Solar Collectors*
Task 4 *Development of an Insolation Handbook and Instrument Package*
Task 5 *Use of Existing Meteorological Information for Solar Energy Application*
Task 6 *Performance of Solar Systems Using Evacuated Collectors*
Task 7 *Central Solar Heating Plants with Seasonal Storage*
Task 8 *Passive and Hybrid Solar Low Energy Buildings*
Task 9 *Solar Radiation and Pyranometry Studies*
Task 10 *Solar Materials R&D*
Task 11 *Passive and Hybrid Solar Commercial Buildings*
Task 12 *Building Energy Analysis and Design Tools for Solar Applications*
Task 13 *Advance Solar Low Energy Buildings*
Task 14 *Advance Active Solar Energy Systems*
Task 16 *Photovoltaics in Buildings*
Task 17 *Measuring and Modeling Spectral Radiation*
Task 18 *Advanced Glazing and Associated Materials for Solar and Building Applications*
Task 19 *Solar Air Systems*
Task 20 *Solar Energy in Building Renovation*
Task 21 *Daylight in Buildings*
Task 23 *Optimization of Solar Energy Use in Large Buildings*
Task 22 *Building Energy Analysis Tools*
Task 24 *Solar Procurement*
Task 25 *Solar Assisted Air Conditioning of Buildings*
Task 26 *Solar Combisystems*
Task 28 *Solar Sustainable Housing*
Task 27 *Performance of Solar Facade Components*
Task 29 *Solar Crop Drying*
Task 31 *Daylighting Buildings in the 21st Century*

Completed Working Groups:
CSHPSS, ISOLDE, Materials in Solar Thermal Collectors, and the Evaluation of Task 13 Houses

To find Solar Heating and Cooling Programme publications and learn more about the Programme visit **www.iea-shc.org** or contact the SHC Executive Secretary, Pamela Murphy, e-mail: pmurphy@MorseAssociatesInc.com

September 2007

What is IEA SHC Task 32

"Advanced Storage Concepts for solar and low energy buildings" ?

The main goal of this Task is to investigate new or advanced solutions for storing heat in systems providing heating or cooling for low energy buildings.

- The first objective is to contribute to the development of advanced storage solutions in thermal solar systems for buildings that lead to high solar fraction up to 100% in a typical 45N latitude climate.

- The second objective is to propose advanced storage solutions for other heating or cooling technologies than solar, for example systems based on current compression and absorption heat pumps or new heat pumps based on the storage material itself.

Applications that are included in the scope of this task include:

- new buildings designed for low energy consumption
- buildings retrofitted for low energy consumption.

The ambition of the Task is not to develop new storage systems independent of a system application. The focus is on the integration of advanced storage concepts in a thermal system for low energy housing. This provides both a framework and a goal to develop new technologies.

The Subtasks are:

- Subtask A: Evaluation and Dissemination
- Subtask B: Chemical and Sorption
- Subtask C: Phase Change Materials
- Subtask D: Water tank solutions

Duration

July 2003 - December 2007.

www.iea-shc.org look for Task32

IEA SHC Task 32 Subtask C
"Storage with Phase Change Materials"

This report is part of Subtask C of the Task 32 of the Solar Heating and Cooling Programme of the International Energy Agency dealing with solutions of storage based on phase change materials or "PCMs".

This reports presents 4 simulation models developped in Task 32 to analyze systems with PCM storage.

Projects presented in this report reflects the knowledge of the participating body presenting the project.

Task 32 Subtask C participants can be proud of having succeeded in providing validated tools to be used within TRNSYS for future work on PCM in tanks.

The Operating Agent would like to thank the authors of this document for their implication in the search of future storage solutions for solar thermal energy, the key to a solar future for the heating and cooling of our buildings.

Jean-Christophe Hadorn

Operating Agent of IEA SHC Task 32
for the Swiss Federal Office of Energy

BASE Consultants SA - Geneva
jchadorn@baseconsultants.com

Contents

INTRODUCTION

PCM-stores are described since a long time in literature and various configurations have been tested under laboratory conditions as well as outdoor conditions. Nevertheless a comparison to water stores was done very seldom. This comparison can only be done, if identical systems are tested back to back with a PCM store and a water store or via simulation. The latter is the far simpler and cheaper solution and additionally offers the possibility to optimize hydraulics and control for both storage types for a given application.

In the beginning of the Task 32 no suitable simulation models for PCM stores were available. Therefore three groups started to develop numerical models for PCM stores that can be used in the simulation environment TRNSYS. With these models there is now the opportunity to develop optimized systems with various PCM store, hydraulic and control configurations.

At HEIG-VD in Yverdon-les-Bains, Switzerland a PCM model using the TRNSYS standard Type 60 as basis was developed for different shapes (plates, cylinders and spheres) and numbers of PCM modules in the tank (Type 860). Additionally subcooling, hysteresis and convection of the liquid part of the PCM in the modules was modeled. The type of PCM is modeled using a temperature-enthalpy curve defined by 5 points.

At the Institute of Thermal Engineering (IWT), Graz University of Technology, Austria a new type for a heat storage including pure water, PCM slurries, PCM modules (plates, cylinders and spheres), subcooling and hysteresis was developed (Type 840). The PCM type is given by an ASCII-Input file that is read by the module. Instead of water a PCM slurry can be used as the storage medium.

Another store model for an immersed heat exchanger (finned air to water type) in a PCM filled tank was developed at IWT for the simulation of applications with high requirements concerning the charging and discharging power with little temperature loss (Type 841).

At BYG DTU, Department of Civil Engineering a PCM store model for long term storage of subcooled PCM in different compartments was developed and validated against laboratory measurements (Type 185).

All models are described in the following

1 SIMULATION MODEL OF PCM MODULES PLUNGED IN A WATER TANK (TYPE 860)

Jaques Bony, Stephane Citherlet., HEIG-VD, Yverdon-les-Bains, Switzerland,

1.1 INTRODUCTION

This paper describes the numeric model developed to simulate heat transfer in phase change materials (PCM) plunged in water tank storage. This model, based on the enthalpy approach [1], takes into account the conduction and the convection into PCM as well as at the interface between PCM and water of the storage. Hysteresis, subcooling and convection are also taken into account. This model has been implemented in an existing TRNSYS type of water tank storage (type 60) [2]. It allows the simulation of a water storage tank filled with PCM modules made of different materials and different shapes such as cylinders, plates or spheres bed. Comparisons between measurements and simulations has been undertake to evaluate the potential of this model.

1.2 Nomenclature

A	exchange surface between 2 nodes	[m^2]
A^{PCM}	surface between water and PCM container	[m^2]
Bi	Biot number	[-]
Cp	PCM specific heat	[J/(kg·K)]
Fo	Fourier number	[-]
h^{PCM}	PCM enthalpy	
i	vertical axe (depend of number of water nodes)	[-]
k	horizontal axe (PCM meshing)	[-]
$N^{(modules)}$	number of PCM containers.	[-]
Nu	Nusselt number	[-]
$Q^{(medium)}$	energy of the storage medium of node i	
$Q^{(flow)}$	charging or discharging energy via direct (inlet/outlet) flow including the flow upward and downward in the tank	
$Q^{(hx)}$	heat flux through internal heat exchanger	
$Q^{(aux)}$	auxiliary energy	
$Q^{(cond)}$	thermal conduction to neighboring nodes	
$Q^{(loss)}$	thermal losses through the tank envelope to the ambient	
$Q^{(modules)}$	energy exchange between the storage medium and PCM modules	
Ra	Rayleigh number	[-]
t	time step simulation	[s]

t_0	initial time	[s]
t_1	final time	[s]
T	storage medium temperatures (node i)	[°C]
T^{PCM}	surface temperature of PCM container	[°C]
U	heat transfer coefficient water/PCM.	[W/(m^2·K)]
x	distance between 2 nodes	[m]
α	convective coefficient between water and PCM	[W/(m^2·K)]
λ	PCM thermal conductivity	[W/(m·K)]
λ_{eff}	effective thermal conductivity	[W/(m·K)]
ρ	PCM density	[kg/m^3]

1.3 GENERAL DESCRIPTION

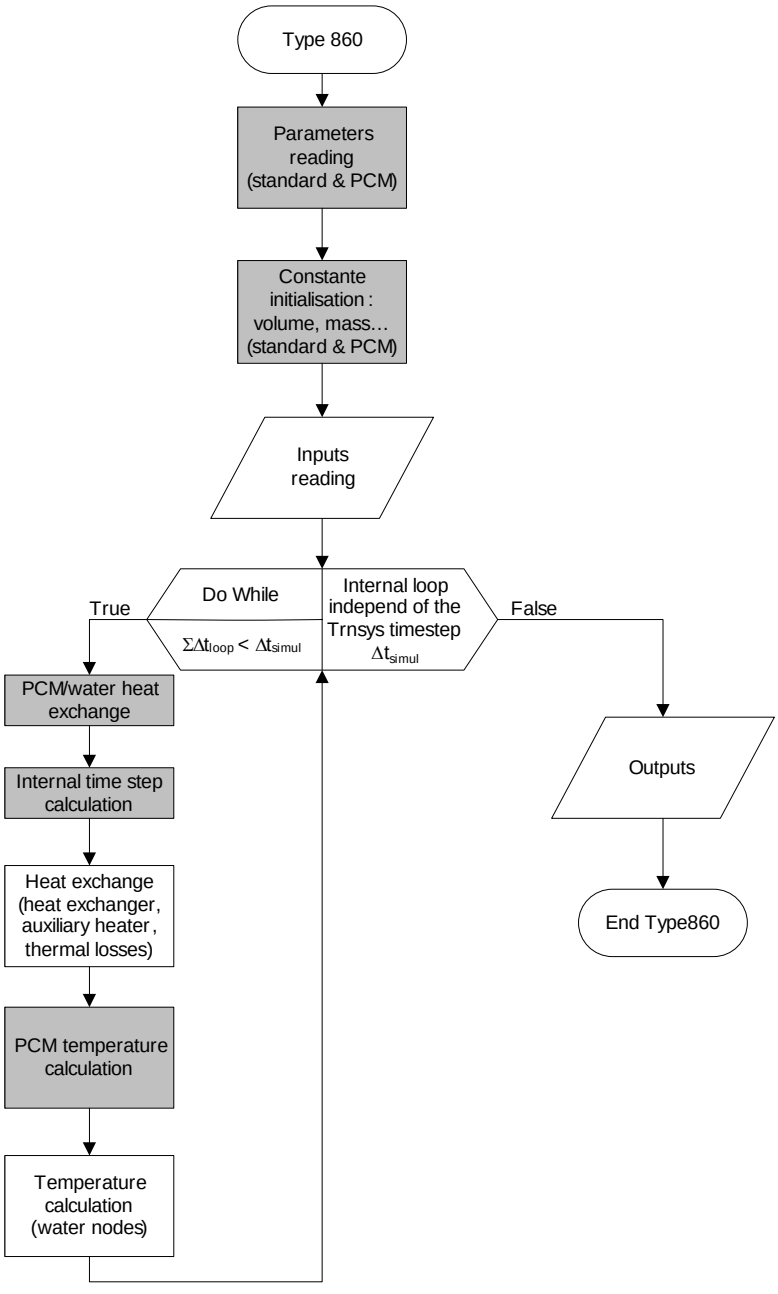

The developed model is an extension of the existing TRNSYS Type 60, for stratified fluid tanks based on sensible energy storage only. The tank can be made up to 100 fully mixed nodes. The number of nodes determines the degree of calculation accuracy. It can be improved with the increase of the node number. The initial maximum node number of 100 in the type 860 has been augmented up to 400. Furthermore, this model has been adapted to be able to take into account the PCM calculation (Figure 1).

Figure 1 : Diagram of PCM model adaptations into the standard type60 TRNSYS.

Figure 2 shows the different heat fluxes of the energy balance considered in each node of the water tank. For each node, the temperature is assumed to be uniform.

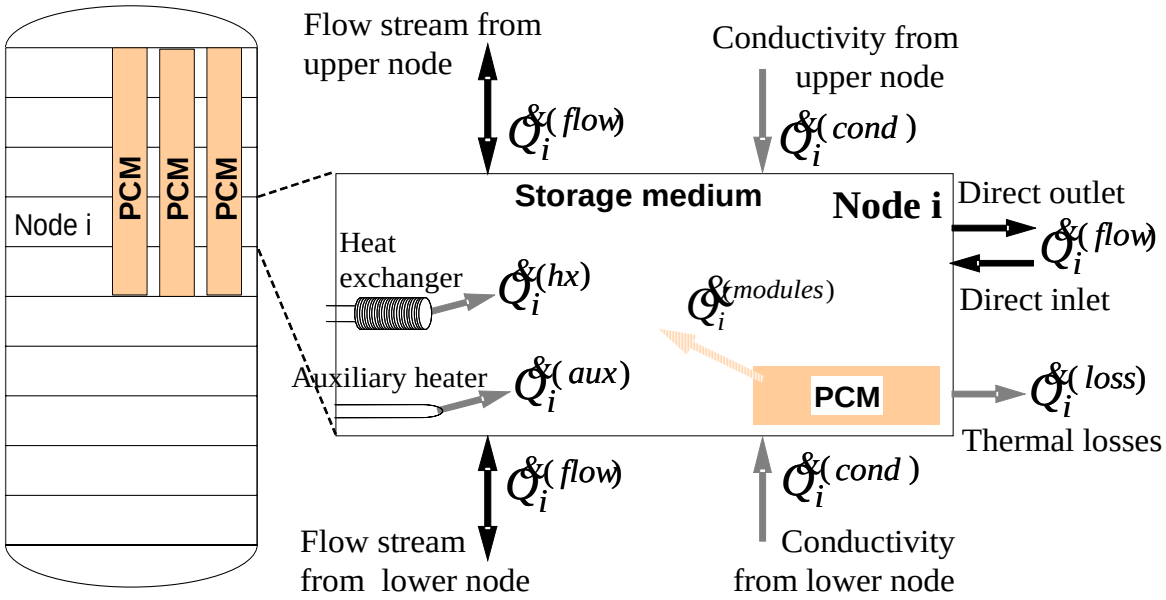

Figure 2 Tank node system and energy balance for each i_{th} water node

According to the notation in Figure 2, for each ith node, the energy balance is defined by the following equation:

$$\dot{Q}_i^{(medium)} = \dot{Q}_i^{(flow)} + \dot{Q}_i^{(hx)} + \dot{Q}_i^{(aux)} + \dot{Q}_i^{(cond)} + \dot{Q}_i^{(loss)} + \dot{Q}_i^{(modules)} \qquad (1)$$

The energy exchange between the storage medium and the PCM modules is governed by the following equation (Bony et al. 2005):

$$\dot{Q}_i^{(modules)} = -N^{(modules)} \left\{ U_i A_i^{PCM} \cdot \left[T_i - T_i^{PCM}\left(h_i^{PCM}\right) \right] \right\} \qquad (2)$$

The calculation of heat transfer through the PCM uses the enthalpy method, which means that for a given volume and material, a continuous and reversible function, can be calculated which will return the temperature *T* depending on the calculated enthalpy *h*. This temperature is used during the simulation to determine the node temperature, according to the enthalpy of the system at time *t*. Figure 3 shows this function which is modeled by a succession of 5 straight lines: two for the sensible heat in solid or liquid phase and three straight lines in the phase change part. This leads to a sufficient accuracy for the calculations.

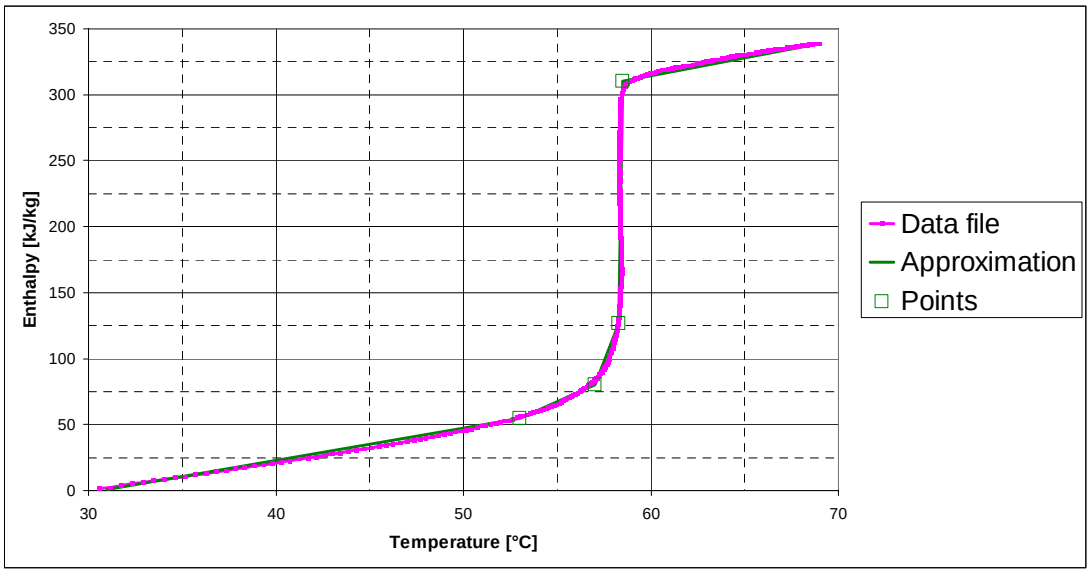

Figure 3 : Example of an enthalpy curve for a particular volume and PCM type.

1.3.1 PCM meshing

The internal calculation model in the PCM is bi-dimensional, which allows the simulation of different PCM shapes: cylinder, sphere or plate. An onion peel approach has been used. It consists of representing a PCM element by a succession of constant thickness layers whose shape depends on the object, as shown in Figure 4.

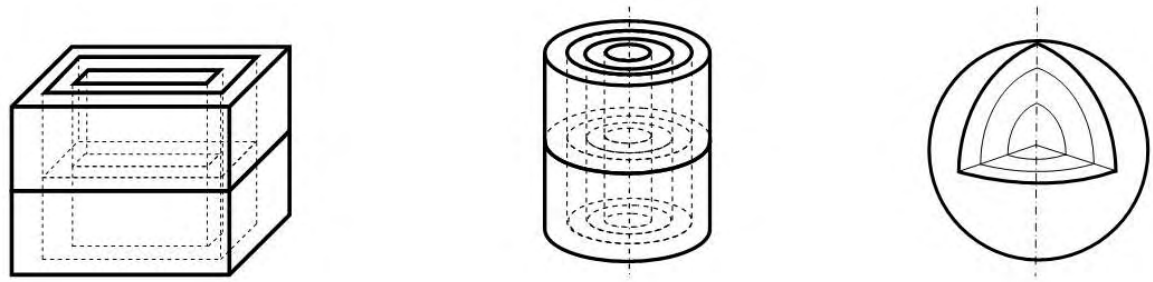

Figure 4 Representation of the shapes available in the adapted TRNSYS model

For each node, we calculate the energy balance while supposing a uniform temperature in the volume of the corresponding node (Figure 5), which has an enthalpy variation given by the equation (3):

$$\frac{\Delta h^{t1}{}_{i,k}}{\Delta t} = \dot{Q}^{t1}_{i,k-1\to i,k} + \dot{Q}^{t1}_{i,k+1\to i,k} + \dot{Q}^{t1}_{i-1,k\to i,k} + \dot{Q}^{t1}_{i+1,k\to i,k} \qquad (3)$$

Where the heat transfer at water-PCM interface (k=1) is:

$$\dot{Q}^{t1}_{i,Water\to i,k} = h_{i,Water\to i,k} \cdot A_{i,Water\to i,k} \cdot \left(T^{t0}_{i,Water} - T^{t0}_{i,k}\right) \qquad (4)$$

Where the heat transfer between 2 nodes of PCM is:

$$\dot{Q}^{t1}_{i,k-1\to i,k} = \left(\frac{\lambda_{eff,i,k}}{x_{i,k}} + \frac{\lambda_{eff,i,k-1}}{x_{i,k-1}} \right) \cdot A_{i,k-1\to i,k} \cdot \left(T^{t0}_{i,k-1} - T^{t0}_{i,k} \right) \quad (5)$$

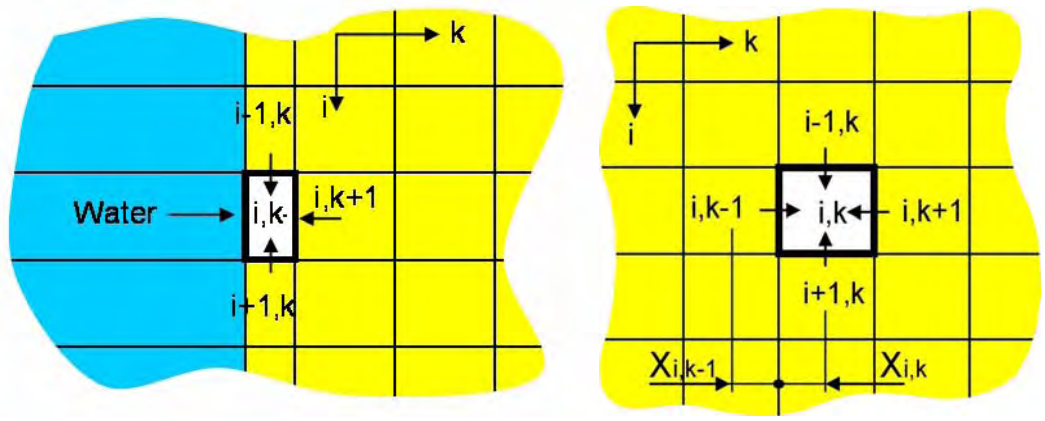

Figure 5 PCM mesh at the water-PCM interface and inside the material

1.3.2 Heat Transfer

1.3.2.1 Water / PCM convection

The convective coefficient between the water of the tank storage and the PCM container is calculated for every node and each time step, according to the container shape chosen:

Plate and cylinder → vertical plate convection [4]

Sphere → convection around a sphere in free convection and in a sphere bed in forced convection [5] [6].

Table 1 gives the different equations of the convective coefficient used according to the shape of the PCM module as well as the type of fluid flow around these modules [4] [5].

Table 1 Equations for water / PCM convection.

Convection	**Vertical plate ou cylinder**	**Sphere bed**
Laminar free Turbulent free	$Nu = \left\{ 0.825 + \frac{0.387 \cdot Ra^{1/6}}{\left[1 + (0.492/\mathrm{Pr})^{9/16}\right]^{8/27}} \right\}^2$	$Nu = 2 + 0.56\left(\frac{\mathrm{Pr}}{0.846 + \mathrm{Pr}} Ra \right)^{1/4}$ (Ra<10^{11})
Laminar Forced	$Nu_x = 0.332 Re_x^{1/2} \cdot Pr^{1/3}$ (Re<5.10^5)	$Nu_{laminar} = 0.664 \cdot (Re/\varepsilon)^{1/2} \cdot Pr^{1/3}$ $Nu_{turbulent} = \frac{0.037(Re/\varepsilon)^{0.8}\,\mathrm{Pr}}{1 + 2.443(Re/\varepsilon)^{-0.1}(\mathrm{Pr}^{2/3} - 1)}$ $Nu_{Global} = 2 + (Nu_{laminar}^2 + Nu_{turbulent}^2)^{1/2}$ $Nu = (1 + 1.5(1-\varepsilon)) \cdot Nu_{Global}$ (ε= void fraction in sphere bed)
Turbulent Forced	$Nu_x = 0.0296 Re_x^{4/5} \cdot Pr^{1/3}$ (5.10^5<Re<10^7)	

Where mixed Nusselt number and convective coefficient calculation with free and forced (water flow into tank storage) convection are given by [4]:

$Nu_{Mixed}=(Nu_{Free}^{3}+Nu_{Forced}^{3})^{1/3}$ [-] (6)

$$\alpha = \frac{Nu_{Mixed} \cdot \lambda}{x}$$ [W/m^2.K] (7)

1.3.2.2 Thermal conduction inside PCM in solid or liquid phase

In order to take into account the thermal conduction difference between the solid and liquid states of a material, the model allows 2 distinct values for the conduction coefficient; one for the solid and one for the liquid phase.

At the time of the phase change, the thermal conductivity value is calculated by linear interpolation of the enthalpy (Figure 6).

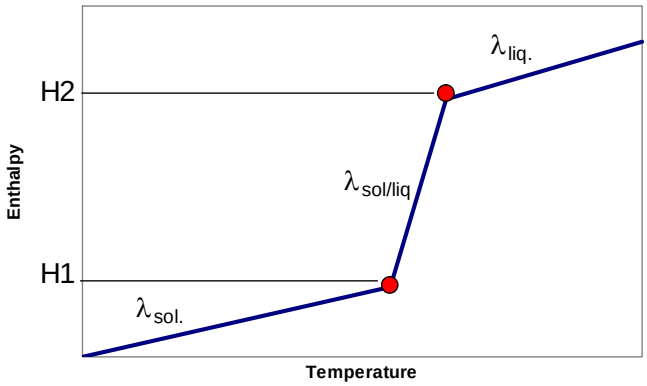

Figure 6 : Calculation of the thermal conductivity λ in accordance to the enthalpy H.

Below the enthalpy value H1, the thermal conductivity λ is constant and equal to λ_{sol}. Above the enthalpy value H2, the thermal conductivity is constant and is equal to λ_{liq}. Between H1 and H2, the conductivity is given by linear interpolation:

$$\lambda_{sol/liq} = \lambda_{sol} + \frac{\left(\lambda_{liq} - \lambda_{sol}\right)}{\left(H2 - H1\right)}\left(h^{t} - H1\right)$$ (8)

Where, h^t is the enthalpy value at time step t.

1.3.2.3 Effective thermal conductivity

In order to take into account of the convection in the liquid PCM, an effective thermal conductivity has been included, which is given by:

$$\lambda_{eff} = \lambda \cdot Nu$$ (9)

Where, Nu = Nusselt number for internal convection.

Several equations exist to define convection inside cavities (Nusselt number). The cavity size, with its natural convection, influences the value of the convection coefficient. It would be necessary to take into account the height and the width of the cavity.

However, some equations don't use height notion for the convective cell, which simplifies its implementation in the calculation (Equations (10) and (11)).

The Nusselt number calculation used in the model is:

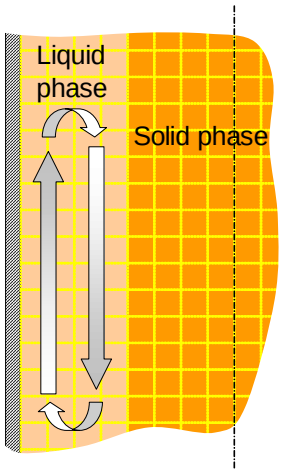

Figure 7 : Calculation

1) Rectangular / cylindrical cavity: $10^6 < Ra < 10^9$ [4]

$$Nu = 0.046 Ra^{1/3} \quad [-] \qquad (10)$$

2) Spherical cavity: $10^2 < Ra < 10^9$ [7]

$$Nu = 0.228\, Ra^{0.226} \quad [-] \qquad (11)$$

The validity range is for a ratio height/width between 1 and 40 for liquid. These values seem large enough to be used in a PCM module. Thus, we concentrated on the thickness determination of the liquid PCM layer to define the number of Nusselt in every node. Besides, during a thermal cycle, it is possible to have several liquid layers separated by a solid PCM layer.

To evaluate the conformity of the model, different experiments have been undertake with different PCM shapes like a cylinder or a sphere bed, and different PCM types like paraffin or sodium acetate trihydrate. Results have shown a good agreement between simulations and experiments [10].

1.3.3 Simulation time step

The numerical resolution of the equations set can be done by an explicit or implicit method. The explicit method is simple to program but is conditionally steady. It needs to have a time step smaller than a limit value. The implicit method is more complex to program but it is unconditionally steady. There is no limit for the time step except if we would like good calculation accuracy.

As the explicit method has been chosen, it is necessary to pay attention to the time step in order to avoid a calculation divergence. The criteria of convergence are calculated with the following equations [4]:

- for the interface water/PCM

$$Fo\left(2+Bi\right)\leq 1/2 \qquad (12)$$

- for a node inside PCM material

$$Fo\leq 1/4 \qquad (13)$$

$$Fo=\frac{\lambda\cdot t}{\rho\cdot Cp\cdot x^2} \quad \text{et} \quad Bi=\frac{\alpha\cdot x}{\lambda} \qquad (14)$$

From Equations (15) and (16), we get the maximum time step possible for calculation. It takes into account the heat transfer coefficients (convective PCM/water and conductive) as well as the thermal capacity of every node.

- for interface node water/PCM

$$t\leq\frac{\rho\cdot Cp\cdot x^2}{2\lambda\left(2+\alpha\cdot x/\lambda\right)} \qquad (15)$$

- for a node inside material

$$t\leq\frac{\rho\cdot Cp\cdot x^2}{4\lambda} \qquad (16)$$

1.3.4 Hysteresis

The hysteresis phenomenon appears during the cooling of materials. It results in a delay of the phase change. It doesn't depend on the solid phase presence in the surroundings unlike for subcooling, and therefore this process can be calculated independently for every PCM node.

In order to take into account of the hysteresis, a simple shift of the enthalpy curve according to a differential temperature defined with one parameter, as shown in Figure 8.

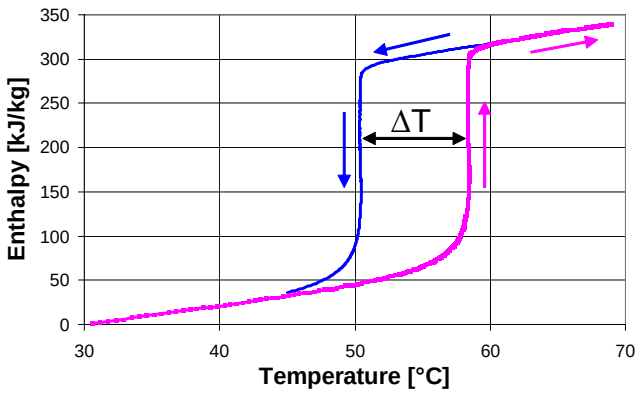

Figure 8 : Hysteresis model

During a heating or cooling step inside the phase change zone, the slope of transition is the same as the solid phase in the bottom part of the phase change. It is also identical to the slope of the liquid phase in the superior part of the phase change. It avoids discontinuity of the enthalpy curve when the transition point is close to the complete phase change (liquid or solid).

1.3.5 Subcooling

Contrary to the previous phenomenon, the subcooling depends on solid phase presence. The determination of this process takes into account the global state of the PCM module. It is necessary that the whole PCM is in liquid phase to obtain subcooling. During the cooling mode, as soon as a PCM part reaches the point of crystallization, the whole PCM will solidify (full line of Figure 9). This phenomenon can start at a lower temperature than the solidification temperature.

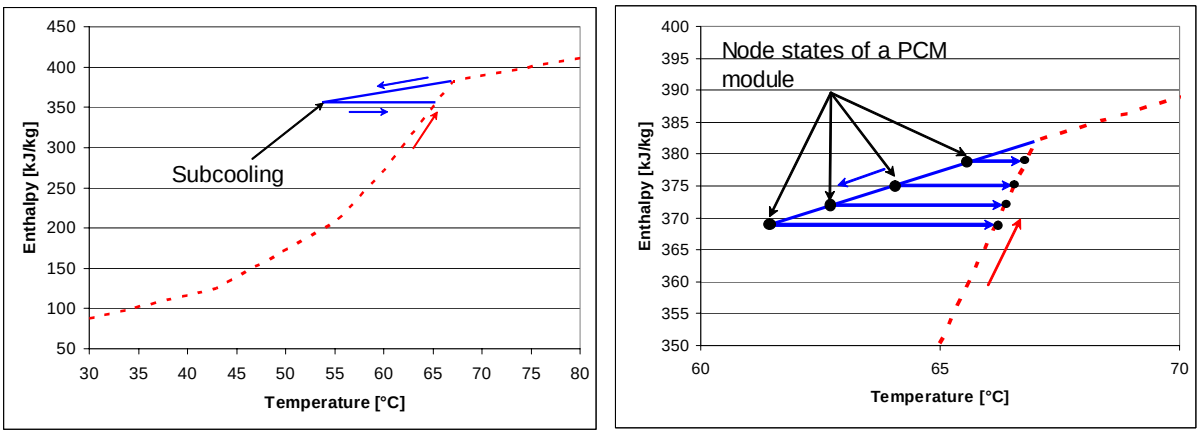

Figure 9 : Subcooling model

Thus, for cylinders or plates, the subcooling will be able to appear only one time during the cooling process. Indeed, when crystallization starts around a condensation core, the solidification propagates in the entire element at a certain speed. In the numerical model, this process is supposed instantaneous, even if it is not the case (Figure 10). But it is difficult to know the crystallization propagation speed in a PCM element. The following figure shows differences between the model and reality. The measurements are made on sodium acetate with graphite during the cooling process.

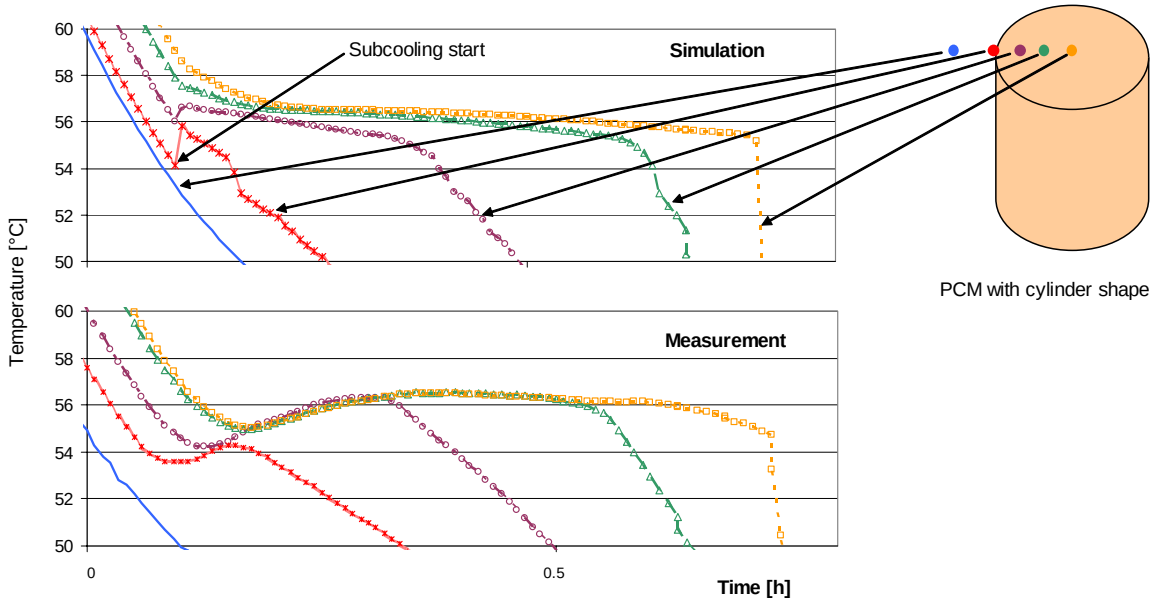

Figure 10 : Comparison between simulation and measurement about crystallization propagation speed

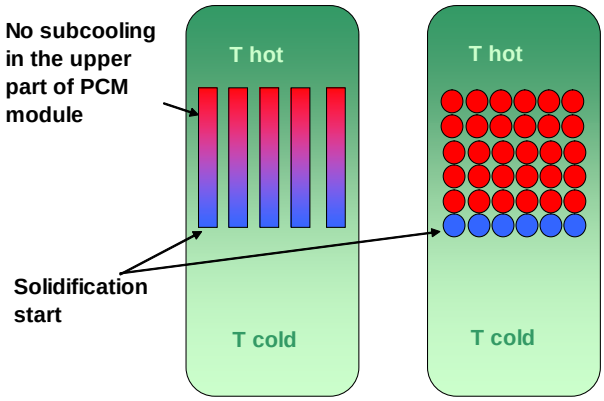

In the spherical module case, this phenomenon will appear at every layer of spheres. Indeed during the thermal discharge, the lower part of the tank storage cools down in first. Thus, the first lower layer of spheres will be in subcooling process whereas the other ones should wait as the tank storage continues to cool down (Figure 11).

Figure 11 : crystallization propagation process according to the container type

The phenomena of hysteresis and subcooling can be combined together as Figure 12 shows. In the model, each of these phenomena is treated independently by a specific state indicator.

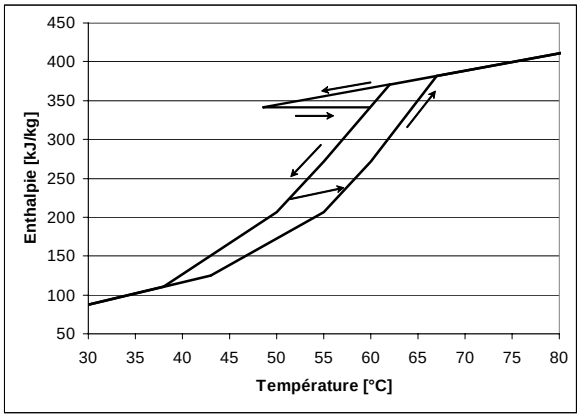

Figure 12 : Combination subcooling and hyteresis

1.3.6 Multi-node

In order to have a good precision of calculations, it is useful to have enough nodes in the water tank storage. Unfortunately, this increase of node number (size reduction of nodes) increases calculation time consuming.

This problem is well known from TRNSYS users. We have to reduce the number of layer in the tank storage, therefore while losing the precision, in order to have reasonable calculation time. For a yearly simulation, it is admitted usually that the node number can be low, about 10 [9], inaccuracies compensating themselves all along the simulation. On the other hand, for calculation on small period, the node number must be higher.

Figure 13 shows with the relation between the number of nodes and the calculation time for the TRNSYS type 60 for a simulation representing 24 hours of real time. We can notice that the TRNSYS model of water tank storage accepts up to 100 nodes in its standard version. For this test, we have increase the maximum number of node until 400.

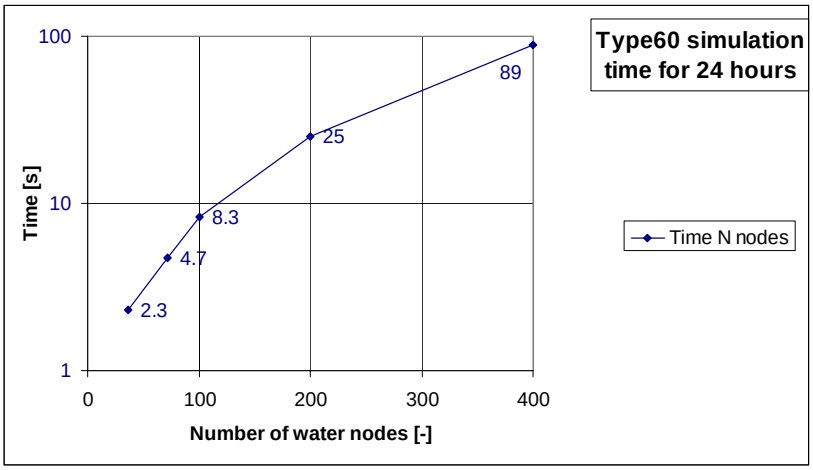

Figure 13 : Increase of time-consuming according to the number of water nodes. Processor used: Pentium4 – 1.6 GHz.

The diagrams of Figure 14 shows the temperatures simulated (dot lines) and measured (full lines) in a water tank for 36, 100 and 400 layers.

The curves represent 9 temperatures at different height in a water tank of 500 litres. The upper part of the tank is set to 63 [°C] and the lower part to 30 [°C]. A cold water at 21 [°C] with a flow rate of 250 [l/h] is injected in the lower part. As shown in Figure 14 the larger the nodes number is the better the simulations fit the experimental results.

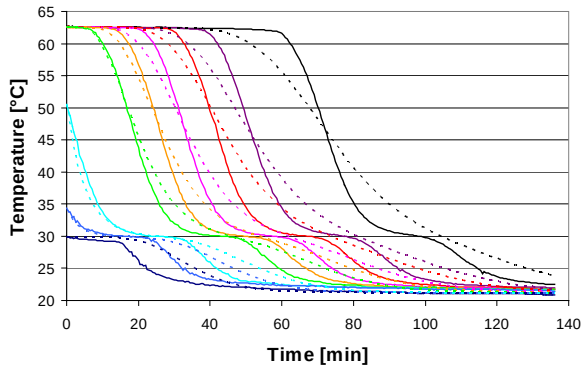

(a) 36 nodes – Time consuming 0.6 [s]

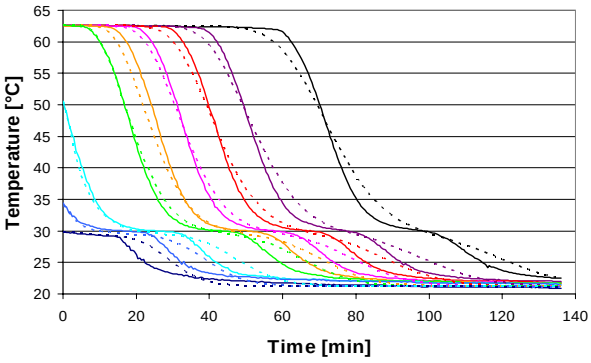

(b) 100 nodes – Time consuming 1,1 [s]

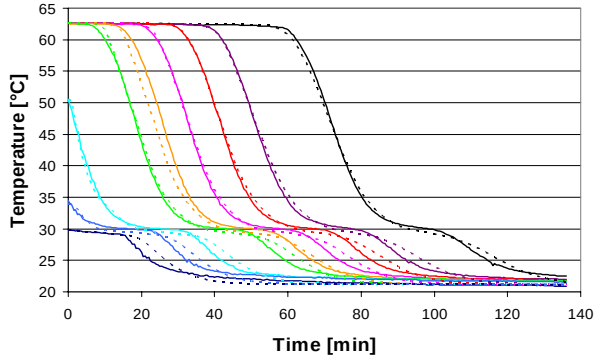

(c) 400 nodes – Time consuming 14 [s]

Figure 14 : Influence of node number increase on result accuracy (type60 TRNSYS).
- full line = experimental data
- dotted line = simulations

Here the meshing of the PCM modules was directly bounded to the vertical nodes number in the water tank storage; for each layer, one node of water was connected with a set of nodes in the PCM as shown in Figure 15. Typically, in a water tank filled with PCM cylinders of 50 [cm] height vertically separated by 10 nodes (1 node for 5 [cm]) and having 10 radial nodes, there is a total of 100 calculations nodes only for the PCM. If to get a better accuracy we increase 5 times the vertical water node number, there will be 500 nodes inside PCM instead of 100. The heat capacity of each node decrease with their size. So, if we increase in one direction (i or k) X time the node number, equations (15) and (16) give and a simulation time step X^2 time smaller (decrease of node size).

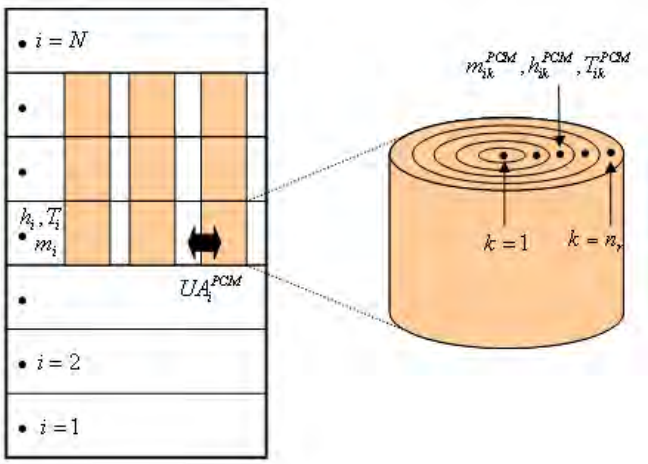

Figure 15 : Classic meshing of calculation node for water and PCM.

In order to improve the simulation accuracy while preserving acceptable calculation time, the idea developed was to dissociate several water nodes to one set of horizontal nodes in the PCM as Figure 16 shows. This solution leads to an important time gain , while keeping a good calculation accuracy

Figure 17 is similar to Figure 13 but for various nodes number.

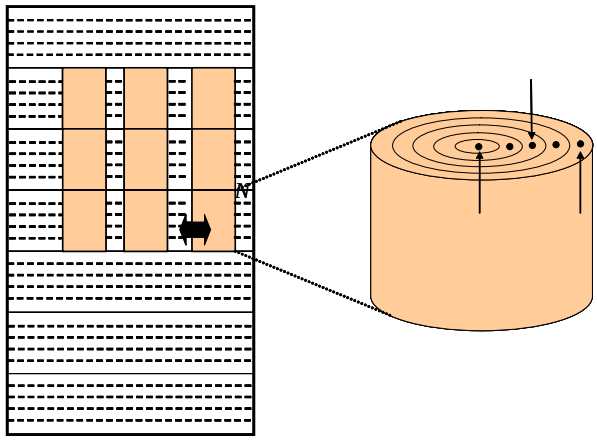

Figure 16 : New meshing of calculation node for water and PCM.

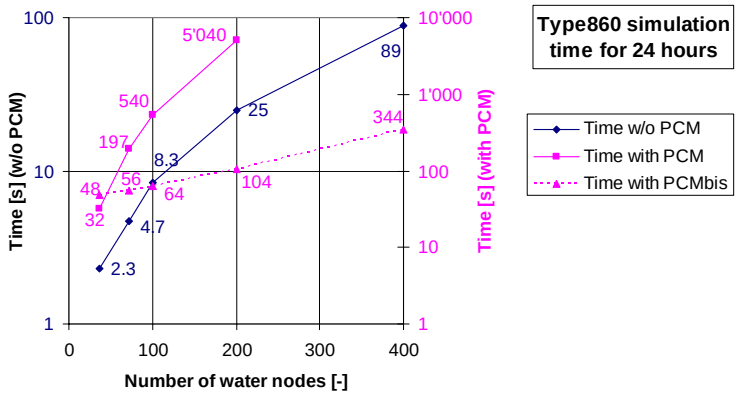

Theses results were obtained with a Pentium processor of 1.6 GHz.

w/o PCM = without PCM

with PCM = with PCM without dissociation water/PCM node

with PCMbis = with PCM used dissociation water/PCM node

Figure 17 : Time-consuming to simulate 24 hours in real time.

As it can be seen, the necessary time, between a water tank without PCM (Time w/o PCM) and with PCM (Time with PCM), is multiplied by a factor between 15 and 20 according to the number of nodes used, what is unacceptable. With the new method of node dissociation used for the PCM (Time with PCMbis) the time is reduced of a factor 50 for 200 water nodes in relation to the method (Time PCM with), value that increases with the node number. These values are only indicative because they depend on the processor type, of the tank type (with or without heat exchanger) and the PCM type took into account.

In addition to the simulation time gain with PCM simulation, this solution has the following advantages for simple water tank storage:

- Possibility to separate a tank in an important number of nodes, for example 200, while only introducing the initial temperatures for 20 layers. Each water layer must be divided by 10. Indeed, with measurements, it is not common to get more than 20 temperatures in a tank. It is arbitrary to define some temperatures for lot of nodes where there is not measurement.
- Possibility to change the water nodes number without change temperature outputs number. So it is easy and fast to visualize its influence thus and to optimize the time consuming.
- Possibility to use several tanks in a same simulation without increasing the 'Derivatives' number (number initial temperatures in TRNSYS) record in file 'param.inc' in TRNSYS14 version.

The problem of increasing the calculation time according to the nodes number (the node size decreases), is exacerbated due to the phase change material (PCM) use. This method of water node dissociation with PCM nodes gives a promising potential.

1.3.7 Type 860 improvement

Some improvements have been introduced in type860 to avoid some mistakes.

1.3.7.1 Heat exchanger energy balance

During the PCM model implementation, the energy balance for heat exchangers has been improved. The heat capacity (Cp) value of fluid at the heat exchanger input is constant (e.g. from a pipe). On the other hand the internal heat transfer calculation is done by the type60 use a non constant value of Cp. This value depends of the fluid temperature. Depending of the fluid inside heat exchanger, the heat capacity value is:

- constant for water Cp_W=4190 [J/kg.K]
- variable for ethylene or propylene glycol as the equation give by the standard type60.

1.3.7.2 Propylene glycol characteristic

For heat exchanger with propylene glycol, it has been notice that the values of fluid dynamic viscosity or fluid thermal conductivity get value which leads to simulation errors. To avoid this problem, limitations are introduced for these two variables. Furthermore, the outlet temperature could not be lower than 10 [°C].

- fluid dynamic viscosity < 0.002 [N.s/m^2] (e.g. value for 35 [°C] and 33% gly)
- fluid thermal conductivity > 0.4+(0.4-gly)*0.005 [W/m^2.K]
  where gly= fraction of glycol concentration
- outlet temperature > 10 [°C]

1.3.7.3 Pi value

The Pi value has been corrected and is now equal to 3.1415926535 in the type860.

1.3.8 Limitations

Of course there are some limitations. The following *Table 2* summarize most of them.

Table 2: Limitations of Type 860.

Limitation	Description
Container shape	Only 3 types of container shape can be used: Plates, spheres and vertical cylinders. For instance, it is not possible to simulate horizontal cylinder.
Height PCM module	Height of PCM module must fit a node height in the water tank. To adjust heights, water nodes can be added.
Subcooling	As in chapter 2.5, subcooling occurs at the same time in whole the PCM zone (except for sphere bed). We could add PCM zone to divide one PCM zone in several zone. Thus subcooling effect occurs at different time.
Number of type860 in simulation	Only one type860 by simulation deck can be used. But type60 can be used in the same deck,

1.4 SPECIFIC PARAMETERS AND OUTPUTS

1.4.1 Specific parameters

In addition to the available parameters in type60, there are 2+40xNz specific parameters for the type 860. Where Nz is the number of PCM zone (10 maximum) inside the water tank.

Two other additional parameters are also used in this model tank\PCM (*Table 3*). One defines the number of PCM module, 10 maximum, and another defines the number of additional water node for each water node available in the base model (see chapter 2.6). Up to 400 nodes can be added (e.g. 10x40 or 5x80) in the model. For example, with 50 initial nodes, it is possible to introduce 8 time additional nodes, to reach 400 nodes. It should be noted that the calculation of heat transfer in the PCM is made from nodes of water at the initial dimension, without taking into account this additional parameter nx. This helps to increase the accuracy of compute the water temperature without increasing significantly the time calculation for PCM simulation.

Table 3: Specific parameter for the type860 model.

N°	Variable name	Description
33	Nz	Number of PCM zone - 10 maximum
34	nx	Node multiplication factor (between 1 and 10). Total water node < 400

Following number of standard parameters must be change by added 2 for each. For example the 33th parameter from the type60 (HX fluid) becomes 35th for the type860.

For the temperature outputs of water node the value is a mean temperature of the nx nodes.

Table 4 explains the different parameters necessary to characterize PCM:

Table 4: Specific parameters for one PCM zone about the type860 model.

N°	**Variable name**	**Description**
1+34+Par(30)*12+ (Nz -1)*40	nodesup(i)	Number of bottom node for each PCM zone
2+34+Par(30)*12+ (Nz -1)*40	nodeinf(i)	Number of top node for each PCM zone
3+34+Par(30)*12+ (Nz -1)*40	PCT1(1,i,j)	Phase Change Temperature for the first point on the enthalpy curve [°C]
4+34+Par(30)*12+ (Nz -1)*40	PCT1(2,i,j)	Phase Change Temperature for the second point on the enthalpy curve [°C]
5+34+Par(30)*12+ (Nz -1)*40	PCT1(3,i,j)	Phase Change Temperature for the third point on the enthalpy curve [°C]
6+34+Par(30)*12+ (Nz -1)*40	PCT1(4,i,j)	Phase Change Temperature for the fourth point on the enthalpy curve [°C]
7+34+Par(30)*12+ (Nz -1)*40	PCT1(5,i,j)	Phase Change Temperature for the fifths point on the enthalpy curve [°C]
8+34+Par(30)*12+ (Nz -1)*40	HH(1, i,j)	enthalpy value for the first point on the enthalpy curve [kJ/kg]
9+34+Par(30)*12+ (Nz -1)*40	HH(2, i,j)	enthalpy value for the second point on the enthalpy curve [kJ/kg]
10+34+Par(30)*12 +(Nz -1)*40	HH(3, i,j)	enthalpy value for the third point on the enthalpy curve [kJ/kg]
11+34+Par(30)*12 +(Nz -1)*40	HH(4, i,j)	enthalpy value for the fourth point on the enthalpy curve [kJ/kg]
12+34+Par(30)*12 +(Nz -1)*40	HH(5, i,j)	enthalpy value for the fifths point on the enthalpy curve [kJ/kg]
13+34+Par(30)*12 +(Nz -1)*40	Hyst(i)	Differential temperature for the Hysteresis phase change during cooling [K]
14+34+Par(30)*12 +(Nz -1)*40	Subcool(i)	Differential temperature of the subcooling phase change[K]
15+34+Par(30)*12 +(Nz -1)*40	Rhol(i)	Average PCM rho. We assume this is a constant value due to the non variable volume of the container [kg/m^3]. This value is used for the enthalpy calculation.
16+34+Par(30)*12 +(Nz -1)*40	Lamb1(i)	Radial solid conductivity into PCM (horizontal heat transfer) [W/m.K]

17+34+Par(30)*12 +(Nz -1)*40	Lamb1Liq(i)	Radial liquid conductivity into PCM (horizontal heat transfer) [W/m.K]
18+34+Par(30)*12 +(Nz -1)*40	Lamb2(i)	Axial solid conductivity into PCM (vertical heat transfer). If this parameter have the same value as the Lamb1(i) parameter, then the thermal conductivity in liquid phase in the axial direction of the PCM module is identical to Lamb1Liq (i) parameter. Otherwise, the axial conduction in liquid or solid phase is the same and equal to the value of this parameter. This parameter allows simulating PCM with graphite plates which have an anisotropic conductivity coefficient. [W/m.K]
19+34+Par(30)*12 +(Nz -1)*40	NcPCM(i)	Number of PCM radial node (include container)
20+34+Par(30)*12 +(Nz -1)*40	Ep0(i)	Thickness of container [mm] (0=no container)
21+34+Par(30)*12 +(Nz -1)*40	Dia(i,1)	Dimension of PCM module [mm] (include container thickness). In case of a rectangular plate, the width and thickness can be made as follows: 350,034 means a width of 350 mm and a thickness of 34 mm. Therefore it is not possible to have a thickness exceeding 999 mm. It is also impossible to have a width with a precision of 0.1 mm.
22+34+Par(30)*12 +(Nz -1)*40	Contain1(i)	Kind of container (1=sphere, 2=cyl. , 3=slab) and void if sphere: In sphere case, we need to define a void fraction. For example 1.286 means a sphere bed with a void fraction of 0.286. Sphere: cubic arrangement, void fraction=0.4764 Sphere: orthorhombic arrangement, void fraction = 0.3954 Sphere: tetragonal arrangement, void fraction = 0.30219 Sphere: rhomboedric arrangement, void fraction = 0.2595 Sphere: random arrangement, void fraction = 0.36 to 0.43
23+34+Par(30)*12 +(Nz -1)*40	Ncont(i)	Number of container in a horizontal cross section. For sphere bed, this parameter is the number of sphere.
24+34+Par(30)*12 +(Nz -1)*40	Rhoc(i)	Container rho [kg/m^3]

25+34+Par(30)*12 +(Nz -1)*40	Cpc(i)	Container Cp [J/kg.K]
26+34+Par(30)*12 +(Nz -1)*40	Lamb0(i)	Container conductivity [W/m.K]
27+34+Par(30)*12 +(Nz -1)*40	KpcmAdd(i)	Additional de-stratification conductivity. It is used if the PCM container is neglected for thermal conduction water / PCM. It takes into account additional conduction between the different nodes of water due to these containers. It is similar to the additional de-stratification conductivity parameter for the whole tank but use only in the PCM zone. [W/m.K]
28+34+Par(30)*12 +(Nz -1)*40	Coeff01(i)	Multiplication factor for convective coefficient between water and PCM. It allows taking into account of eventual fin on the PCM container.
29+34+Par(30)*12 +(Nz -1)*40	TinitPCM(i)	Initial temperature inside the PCM. If this value is zero, then the initial temperature is equal to the water node at the same level.
30+34+Par(30)*12 +(Nz -1)*40	PcmOutput	Number of the PCM node for temperature output. Maximum three nodes by PCM zone. For example: 12.0209 means the 12, 2 and 9 nodes are take into account.
31+34+Par(30)*12 +(Nz -1)*40	Viscocin(i)	Cinematic viscosity of PCM [10^6 m^2/s]
32+34+Par(30)*12 +(Nz -1)*40	Hlimit(i)	Limit enthalpy value from which the PCM is considered in liquid phase [kJ/kg]
33+34+Par(30)*12 +(Nz -1)*40	Rholiq(i)	PCM density in liquid phase [kg/m^3]. This value is used in calculation of effective conductivity coefficient.
34+34+Par(30)*12 +(Nz -1)*40	CpLiq(i)	PCM heat capacity in liquid phase [J/kg.K]
35+34+Par(30)*12 +(Nz -1)*40	CoefDilat(i)	PCM expansion coefficient in liquid phase [1/K]
36+34+Par(30)*12 +(Nz -1)*40	LambLiq(i)	Liquid conductivity into PCM only use for effective conductivity coefficient [W/m.K]
37+34+Par(30)*12 +(Nz -1)*40	Coeff02(i)	Not use
38+34+Par(30)*12 +(Nz -1)*40	Coeff03(i)	Not use
39+34+Par(30)*12 +(Nz -1)*40	Coeff04(i)	Not use
40+34+Par(30)*12 +(Nz -1)*40	Coeff05(i)	Not use

After the PCM parameter, the additional parameter for the node height and the thermal loss coefficient change by adding 40xNz for each. For example with 3 PCM zones and 2 heat exchangers, the 61th parameter from the type60 becomes 181th for the type860.

For height node:
Parameter number = 33+12*Par(30)+2*i+Nz*40 (i=ith water node)

For additional thermal losses:
Parameter number = 34+12*Par(30)+2*i+Nz*40 (i=ith water node)

1.4.2 Specific outputs

The following *Table 5* summarizes the various specific PCM outputs. The output number depends on parameters (number of internal heat exchanger, number of water node). Therefore it is difficult to give precise numbers. However, in the file "fort.1" written by TRNSYS16 (or the file "*.LST" in versions 14 and 15 of TRNSYS), it is possible to read these numbers.

Table 5: Specific outputs for PCM zone in type860.

N°	**Output name**	**Description**
A	PCM temperature	According to the PcmOutput parameter, there are 20 PCM nodes temperature added the surface temperature of the container if there is [°C].
B	Power	For each water node, there is the heat flux going PCM to water [W].
C	Convective coefficient	Convective coefficient between PCM and water for each water node [W/m^2.K]

A -PCM temperature output number = 22+Par(30)*5+n+(i-1)*NcPCM1+1 for the first PCM node and 22+mode5*5+n+i*NcPCM1 for the last PCM node.

Where:

- n = Number of water tank (number of derivative)
- I = ith number of PCM node for output
- NcPCM1 is the maximum number of PCM transversal node for PCM zone: NcPCM1=21 (20 PCM +1 Container)

B and C -There are power and convective coefficient water/PCM for the whole tank nodes. These values are equal to zero in part without PCM.

PCM power output number = 22+Par(30)*5+100+Ncouc*NcPCM1+1
to 22+ Par(30)*5+100+Ncouc*NcPCM1+n

Where:

- Ncouc = Number of PCM node for output

Alpha coeff. between water/PCM = 22+ Par(30)*5+200+Ncouc*NcPCM1+1
to 22+ Par(30)*5+200+Ncouc*NcPCM1+n

1.5 Acknowledgements

We would like to thank our national government: Federal Office of Energy (OFEN/BFE).

We also would like to deeply thank Jean-Christophe Hadorn, representative of the International Energy Agency (IEA) for having initiated the IEA-SHC Task 32.

The IEA Task 32 participants for their collaboration and profitable exchanges.

1.6 References

[1] Visser H., Energy storage in phase-change materials – Development of a component model compatible with the TRNSYS transient simulation program, Delft University of Technology, 1986.

[2] Klein S.A., TRNSYS16 reference manual, 2005.

[3] Bony, J., et al., *Three different approaches to simulate PCM bulk elements in solar storage tank*, PCM2005, Yverdon-les-Bains, June 2005.

[4] Incropera F. P., De Witt D. P., “Fundamentals of heat and mass transfer” Wiley Edition, 1990.

[5] E. Achenbach, *Heat and flow characteristics of packed beds*, Experimental Thermal and Fluid Science, 10:p 17-27, 1995.

[6] Plantier C., Etude numerique et expérimentale d'un prototype de chauffe-eau solaire équipé d'un stockage à changement de phase, Thèse à l'Université de Savoie (France), 2005.

[7] Cengel Y. A., Heat Transfer : A Practical Approach, International Edition, 1997.

[8] Georg Oberndorfer and al., Sensitivity of annual solar fraction of solar space and water heating systems to tank and collector heat exchanger model parameters.

[9] Jokisalo J., et al., *Thermal Simulation of PCM Structures with TRNSYS*, Terrastock 2000, 8th International Conference on Thermal Energy Storage, Stuttgart, Germany, 2000.

[10] Bony, J., and Citherlet, S., Extension of a TRNSYS model for latent heat storage with phase change materials used in solar water tank, Ecostock2006, Stockton.

[11] Bony J. and Citherlet S., Numerical model and experimental validation of heat storage with phase change materials, Energy and Buildings, 2007.

1.7 Annex

Example of a storage tank with 2 PCM zone and 2 heat exchangers written in a deck.

UNIT 12 TYPE 860 T860

PARAMETERS 138

* 1 User-specified inlet positions	* 2 Tank volume
2	1.53
* 3 Tank height	* 4 Tank perimeter
1.8	-1
* 5 Height of flow inlet 1	* 6 Height of flow outlet 1
0.6	0.0
* 7 Height of flow inlet 2	* 8 Height of flow outlet 2
0.	1.8
* 9 Fluid specific heat	* 10 Fluid density
4.19	1000.0
* 11 Tank loss coefficient	* 12 Fluid thermal conductivity
2.34	2.34
* 13 Destratification conductivity	* 14 Boiling temperature
9	120
* 15 Auxiliary heater mode	* 16 Height of 1st aux. heater
2	0.9
* 17 Height of 1st thermostat	* 18 Set point temperature for element 1
1.25	90
* 19 Deadband for heating element 1	* 20 Maximum heating rate of element 1
5	0
* 21 Node containing heating element 2	* 22 Node containing thermostat 2
1	1
* 23 Set point temperature for element 2	* 24 Dead band for heating element 2
55	10.0
* 25 Maximum heating rate of element 2	* 26 Overall loss coefficient for gas flue
0	0
* 27 Flue temperature	* 28 Fraction of critical time step
20	6
* 29 Gas heater?	* 30 Number of internal heat exchangers
0	2
* 31 Node heights supplied	* 32 Additional loss coeff's supplied
1	1

* 2 SPECIFIC PARAMETERS

* 33bis PCM indicator	*33Ter Additional node number by node
2	3

* The following parameter numbers are from the type60

* 33 HX Fluid Indicator-1	* 34 Fraction of glycol-1
1	0.75
* 35 Heat exchanger inside diameter-1	* 36 Heat exchanger outside diameter-1
0.019	0.02

```
* 37 Heat exchanger fin diameter-1          * 38 Total surface area of heat exchanger-1
0.03                                        3
* 39 Fins per meter for heat exchanger-1    * 40 Heat exchanger length-1
0                                           12
* 41 Heat exchanger wall conductivity-1     * 42 Heat exchanger material conductivity-1
55                                          55
* 43 Height of heat exchanger inlet-1       * 44 Height of heat exchanger outlet-1
1.8                                         1.4
*
* 45 HX Fluid Indicator-2                   * 46 Fraction of glycol-2
1                                           0.75
* 47 Heat exchanger inside diameter-2       * 48 Heat exchanger outside diameter-2
0.019                                       0.020
* 49 Heat exchanger fin diameter-2          * 50 Total surface area of heat exchanger-2
0.03                                        3.5
* 51 Fins per meter for heat exchanger-2    * 52 Heat exchanger length-2
0                                           15
* 53 Heat exchanger wall conductivity-2     * 54 Heat exchanger material conductivity-2
55                                          55
* 55 Height of heat exchanger inlet-2       * 56 Height of heat exchanger outlet-2
0.6                                         1.0
*

********************************  PCM  ************************************
* 2x40 SPECIFIC PARAMETERS
*
*
*
* Zone 1
*Nb top node  Nb bot node
4             10
*PCT1 PCT2  PCT3  PCT4  PCT5  HH1   HH2   HH3   HH4   HH5
*PCM54
40    47    49    51    100   80    135   200   290   417
*Hysteres    Subcool      Rhol  Lampcm1     LambLiq     Lampcm2
0            0            900   0.2         0.2         0.2
*Nb pcm node       Thick cont
4                  0
*Dia   Shape       Nb cont      Rhoc  Cpc   Lambda      KpcmAdd
50     2           154          2700  880   200         1.4
*Coeff01     TinitPCM     N° node output
1            0            4.0810
*Viscocin    Hlimit  Rholiq  CpLiq  CoefDilat     LambLiq
5            150     1000    2400   0.001         0.2
* Coeff02     Coeff03      Coeff04      Coeff05
0            0            0            0
*
*
*
* Zone 2
*PCM avec caractéristique carrée
```

*Nb top node Nb bot node
11 17
*PCT1 PCT2 PCT3 PCT4 PCT5 HH1 HH2 HH3 HH4 HH5
*PCM35
24 31 34 37 100 50 100 165 260 417
*Hysteres Subcool Rhol Lampcm1 LambLiq Lampcm2
0 0 900 0.2 0.2 0.2
*Nb pcm node Thick cont
4 0
*Dia Shape Nb cont Rhoc Cpc Lambda KpcmAdd
50 2 154 2700 880 200 1.4
*Coeff01 TinitPCM N° node output
1 0 11.1517
*Viscocin Hlimit Rholiq CpLiq CoefDilat LambLiq
5 150 1000 2400 0.001 0.2
* Coeff02 Coeff03 Coeff04 Coeff05
0 0 0 0
*
*
*
*
********** PCM **********

*Node heights
*Node 1 -Height of node i/Additional loss Node 2 -Height of node i/Additional loss
0.085 0 0.085 0
* Node 3 -Height of node i/Additional loss Node 4 -Height of node i/Additional loss
0.085 0 0.085 0
* Node 5 -Height of node i/Additional loss Node 6 -Height of node i/Additional loss
0.085 0 0.085 0
* Node 7 -Height of node i/Additional loss Node 8 -Height of node i/Additional loss
0.085 0 0.085 0
* Node 9 -Height of node i/Additional loss Node 10 -Height of node i/Additional loss
0.085 0 0.085 0
* Node 11 -Height of node i/Additional loss Node 12 -Height of node i/Additional loss
0.085 0 0.085 0
* Node 13 -Height of node i/Additional loss Node 14 -Height of node i/Additional loss
0.085 0 0.085 0
* Node 15 -Height of node i/Additional loss Node 16 -Height of node i/Additional loss
0.085 0 0.085 0
* Node 17 -Height of node i/Additional loss Node 18 -Height of node i/Additional loss
0.085 0 0.085 0

INPUTS 17
* 1 Flow rate at inlet 1

```
0,0
* 2 Flow rate at outlet 1
0,0
* 3 Flow rate at inlet 2
0,0
* 4 Flow rate at outlet 2
0,0
* 5 Temperature at inlet 1
0,0
* 6 Temperature at inlet 2
0,0
* 7 Environment temperature
0,0
* 8 Control signal for element 1
0,0
* 9 Control signal for element 2
0,0
* 10 Flow rate for heat exchanger -1
0,0
* 11 Inlet temperature for heat exchanger -1
0,0
* 12 Nusselt constant for heat exchanger-1
0,0
* 13 Nusselt exponent for heat exchanger-1
0,0
* 14 Flow rate for heat exchanger -2
0,0
* 15 Inlet temperature for heat exchanger -2
0,0
* 16 Nusselt constant for heat exchanger-2
0,0
* 17 Nusselt exponent for heat exchanger-2
0,0
*** INPUT  VALUES
0 0 0 -2 20 20 15 0.0 0.0 0
20 0.6 0.3 0 5 0.6 0.3

DERIVATIVES 18
50 50 50 50 50 50 50 50 50 50 50 50 50 50 50 50 50 50
```

2 TYPE 840 - MODEL FOR THE TRANSIENT SIMULATION OF WATER- OR PCM SLURRY-TANKS WITH INTEGRATED PCM MODULES

Andreas Heinz, Peter Puschnig, Hermann Schranzhofer
Institute of Thermal Engineering, Graz University of Technology, Austria

2.1 Introduction

The simulation model Type 840 was developed at the Institute of Thermal Engineering within the framework of the European Project PAMELA (2004), the IEA SHC TASK 32 and a national research project (Heinz et al., 2006). The model enables a detailed simulation of water tanks with integrated PCM modules of different geometries (cylinders, spheres and plates) or tanks filled with PCM slurry.

2.2 General description of the model

Since the thermal properties of a phase change material (PCM) change more or less rapidly during a phase change, and in particular the latent heat of the phase change must be accounted for, the modeling of the thermal processes during a phase change requires a general theoretical approach. For this storage model the so called enthalpy approach (Claußen, 1993), (Visser, 1986) is used, in which the enthalpy is a continuous and invertible function of the temperature. Under this assumption one can formulate an energy balance equation for each storage node, from which the time evolution of the enthalpy and – via the unique enthalpy-temperature relation – also the temperature evolution for each node can be calculated.

2.3 Governing equations

The thermal modeling of the PCM storage tank has been implemented as a multi-node storage model into the simulation environment TRNSYS 16. As shown in Figure 18 the storage volume is divided into N horizontal segments (nodes) each characterized by the enthalpy h_j, the temperature T_j and the mass m_j of the storage fluid in the node (j). The energy balance equation for each storage node leads to the time evolution of the enthalpy h_j and via the unique relation h=h(T) also to the temperature T_j of a given node:

$$m_j \frac{h_j^{p+1} - h_j^p}{\Delta t} = \dot{Q}_{dp}^p + \dot{Q}_{hx}^p + \dot{Q}_{aux}^p + \dot{Q}_{cond}^p + \dot{Q}_{loss}^p + \dot{Q}_{module}^p \quad (1)$$

The left side of the equation describes the evolution of the enthalpy in the node (j) from the previous time step (p) to the new time step (p+1), where Δt is the size of the time step. The right side expresses the heat flows in and out of the respective node. (dp) denotes the heat flow due to the mass flow through a double port (=direct connection to the tank), (hx) is the heat exchange with an internal heat exchanger, (aux) the heat input from a built-in auxiliary heater, (cond) the heat conduction to adjoining storage nodes, (loss) the losses to the ambient and (module) the heat exchange with built-in PCM modules. The calculation of the individual terms is done according to the equations described in the following.
The evolution of the enthalpy with time is determined with the so-called explicit approach:

$$h_j^{p+1} = h_j^p + \frac{\Delta t}{m_j} \sum \dot{Q}^p \qquad (2)$$

Thus the enthalpy in the time (p+1) results explicitly out of the respective terms in the time (p).

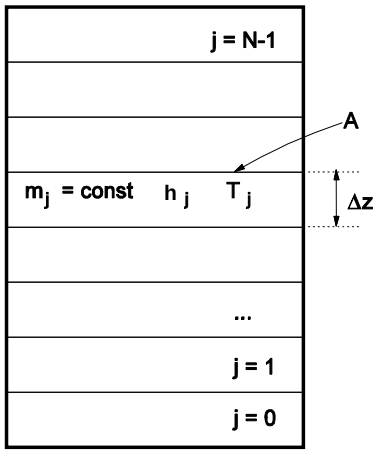

Figure 18: Multi-node storage model with N nodes with the height Δz and the top and lower cross sectional area A; the j^{th} node has the mass m_j the enthalpy h_j and the temperature T_j

2.3.1 Direct connections (double ports)

The storage tank model allows up to five direct hydraulic connections to the tank, so-called double ports. For each of these double ports (c), the mass flow $\dot{m}_{c_{in}}$ and the enthalpy $h_{c_{in}}$ at the inlet are specified as input values for the storage tank. The respective heat flow in or out of node (j) is determined according to

$$\dot{Q}_{dp_j} = \sum_c \dot{m}_{c_{in}} \left(\left(h_{c_{in}} - h_j \right) d_{i_c,j} + \left(h_{j+d_c} - h_j \right) e_{i_c,j,o_c} \right) \qquad (3)$$

$$\dot{Q}_{dp_j} = \sum_c \dot{m}_{c_{in}} \left(\left(h_{c_{in}} - h_j \right) d_{i_c,j} + \left(h_{j+d_c} - h_j \right) e_{i_c,j,o_c} \right) \qquad (4)$$

The nodes at the inlet and the outlet of the double port are denoted by i_c and o_c respectively, as indicated in Figure 19. $d_{i_c,j}$ ensures that the heat flow from the inlet of the double port is added to the node at the inlet i_c:

$$d_{i_c,j} = \begin{cases} 1 \text{ if } i_c = j \\ 0 \text{ if } i_c \neq j \end{cases} \qquad (5)$$

d_c defines the direction of the heat flow (upwards or downwards) with

$$d_c = \begin{cases} +1 \text{ if } i_c \geq o_c \\ -1 \text{ if } i_c < o_c \end{cases} \qquad (6)$$

and e_{i_c,j,o_c} ensures that the heat flow associated with the double port is exchanged only between the nodes delimited by i_c and o_c:

$$e_{i_c,j,o_c} = \begin{cases} 1 \text{ if } 0 < d_c(i_c - j) \leq d_c(i_c - o_c) \\ 0 \text{ else} \end{cases} \quad (7)$$

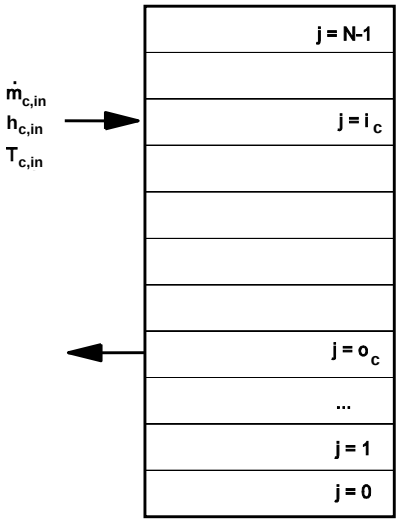

Figure 19: Multi-node storage model with a direct connection (double port) (c); the inlet is located at the node i_c, the outlet at the node o_c

2.3.2 Internal heat exchangers

For the modeling of the charging and discharging processes via internal heat exchangers the heat exchanger is also subdivided into several nodes with a certain mass, enthalpy and temperature, as shown in Figure 20. Up to five heat exchangers can be used in the model.

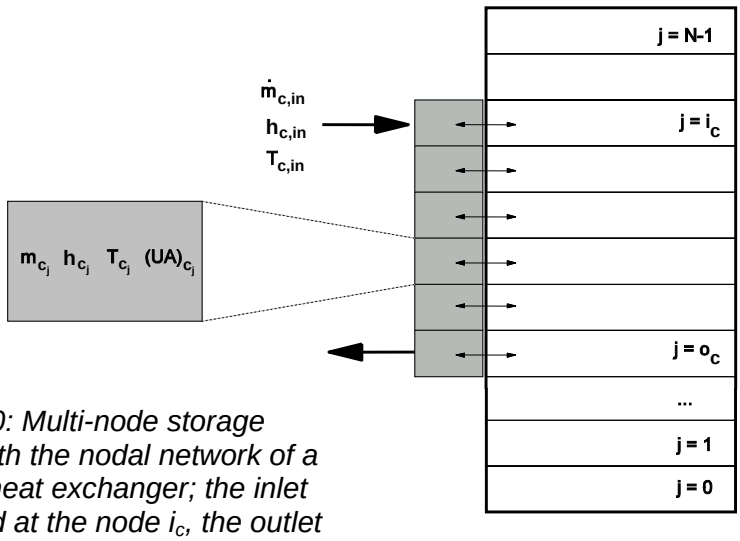

Figure 20: Multi-node storage model with the nodal network of a internal heat exchanger; the inlet is located at the node i_c, the outlet at o_c

The energy balance of the storage node (j) has to be solved together with the energy balance of the heat exchanger node (j). If the heat transfer per temperature difference

between the storage node (j) and the corresponding node of the heat exchanger (c) is denoted as $(UA)_{c,j}$, then the heat flow is calculated with equation (8).

$$\dot{Q}_{hx,j} = \sum_{c} (UA)_{c,j} (T_{c,j} - T_j) \quad (8)$$

T_j and $T_{c,j}$ are the temperatures of node (j) of the storage and the heat exchanger (c) respectively. The energy balance of the heat exchanger node has a similar form as equation (3) with an additional term that describes the heat transfer to the storage node.

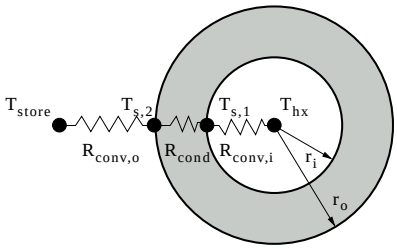

Figure 21: cross section through a heat exchanger tube with inner radius r_i and outer radius r_o; the different thermal resistances are indicated

The heat transfer coefficient $(UA)_{c,j}$ is calculated as a function of the sum of the inner and outer resistances to convective heat transfer and the thermal resistance of the tube wall (see Figure 21).

$$R_{tot} = \frac{1}{\alpha_i 2\pi r_i L} + \frac{\ln(r_o / r_i)}{2\pi \lambda L} + \frac{1}{\alpha_o 2\pi r_o L} \quad (9)$$

The calculation of the convective heat transfer on the inner side is done according to empirical relations for the flow in circular tubes. The convective heat transfer coefficient on the outside of the tube α_o can be calculated according to two different empirical approaches (VDI, 1997) or a fixed value can be provided by the user.

2.3.3 Electrical auxiliary heater

If the electrical power P_j is added the storage node j, then equation (10) applies.

$$\dot{Q}_{aux,j} = P_j \quad (10)$$

2.3.4 Heat transfer by conduction to adjoining nodes

The enthalpy change of the storage node (j) because of heat conduction to the adjoining nodes (j+1) and (j-1) is determined with the following equation:

$$\dot{Q}_{cond,j} = \lambda_{eff} \frac{A}{\Delta z} (T_{j+1} + T_{j-1} - 2T_j) \quad (11)$$

The effective vertical thermal conductivity λ_{eff} has to be provided by the user. It considers the intrinsic thermal conductivity of the storage fluid, increased because of the thermal conductivity of the storage envelope and e.g. internal heat exchangers. A and Δz denote the cross sectional area and the height of the storage nodes respectively.

2.3.5 Heat losses to the ambient

The heat loss of the node (j) with the temperature T_j to the ambient with the temperature T_{amb} is calculated according to equation (12).

$$\dot{Q}_{loss,j} = (UA)_{loss} (T_{amb} - T_j) \quad (12)$$

The heat transfer coefficient $(UA)_{loss}$ can be provided by the user as a fixed value or as a function of the temperature difference (linear dependence).

2.3.6 Heat exchange with built-in PCM modules

In addition to the possibility of using PCM slurries as the storage fluid, the model allows the simulation of built-in PCM modules. Three different PCMs can be integrated into 3 different zones defined by the user (compare Figure 22).

In the current version of the model three module geometries are possible. Cylinders, spheres and plates filled with PCM can be integrated into the tank. Instead of simple cylindrical rods also cylindrical pipes can be simulated (see Figure 23). The module geometries (length, diameter or thickness, wall thickness of the module) and the thermal properties of the PCM material are provided by the user.

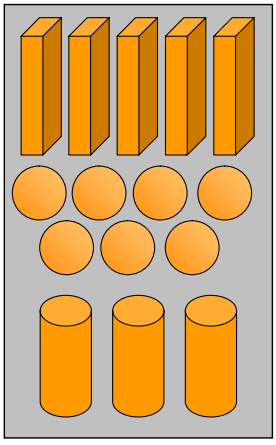

Figure 22: Storage tank with three different PCM zones; a different PCM can be defined for each zone, three different module geometries are possible: plates, spheres and cylinders

The model calculates the heat transfer between the storage fluid and the PCM modules and the heat transfer inside the PCM modules by conduction as well as the phase change processes. Depending on the geometry the modules are subdivided into a 1-dimensional

(spheres) or 2-dimensional (cylinders, plates) nodal network. Thereby the energy balance of each node has to be solved in every time step, considering the conduction processes between the different PCM nodes. The energy balance of an inner node in a cylindrical module is formulated according to equation (13). The heat transfer inside of the module is calculated only by conduction, convection effects in the liquid phase of the PCM are not considered. For the nodes at the surface of the module the equation looks a bit different, since radial and/or axial conduction occurs only with one adjoining PCM node. Additionally the heat exchange with the surrounding water has to be accounted for.

$$m_{PCM_{k,j}} \frac{h_{PCM_{k,j}}^{p+1} - h_{PCM_{k,j}}^{p}}{Dt} = V_{PCM_{k,j}} l_{PCM} \left[\frac{T_{PCM_{k,j-1}} - 2T_{PCM_{k,j}} + T_{PCM_{k,j+1}}}{(Dz)^2} \right] + V_{PCM_{k,j}} l_{PCM} \left[\frac{r_{k+1}\left(T_{PCM_{k+1,j}} - T_{PCM_{k,j}}\right) + r_k \left(T_{PCM_{k-1,j}} - T_{PCM_{k,j}}\right)}{r_{(k+1/2)} (Dr)^2} \right] \quad (13)$$

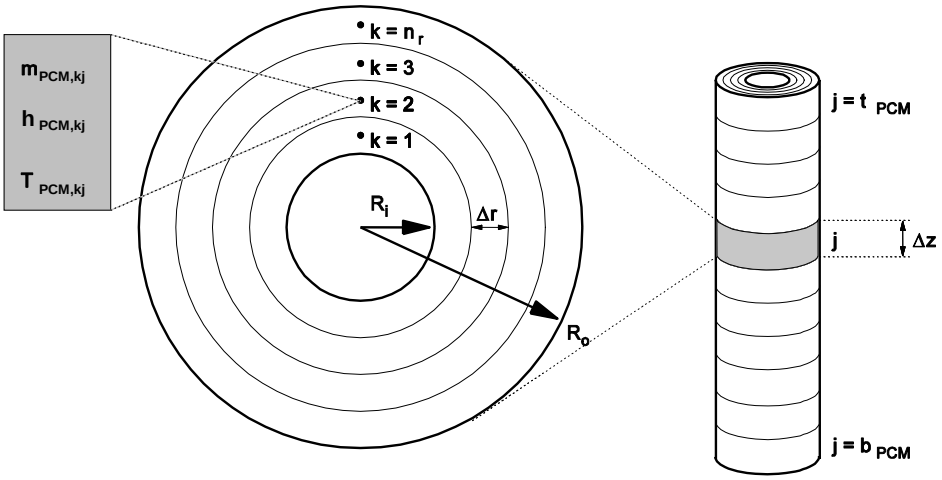

Figure 23: Nodal network of a cylindrical PCM module (pipe module) with the vertical nodes (j) and the radial nodes (k)

2.4 Implementation of the thermal properties of the PCM materials

The thermal properties of the PCM materials are read from ASCII data files. The enthalpy h, the density ρ and the thermal conductivity λ of the materials have to be provided as a function of the temperature. For the storage medium (water or PCM slurry) also the viscosity as a function of temperature is necessary in order to enable an accurate calculation of the convective heat transfer. A maximum of 100 values for 100 different temperatures can be given. The properties in-between these values are determined by means of linear interpolation. Figure 24 shows an example for a material data file.

Material data (h, ρ, λ, μ)

#Temp[°C]	h[J/kg]	rho[kg/m^3]	lam[W/mK]	mu[N s/m^2]
0.00	0.0	996.0	0.25	21.4237e-3
5.00	18837.5	994.0	0.25	18.2852e-3
10.00	37675.0	992.0	0.25	15.5937e-3
15.00	56512.5	990.0	0.25	13.3047e-3
20.00	75350.0	988.0	0.25	11.3758e-3
35.07	132450.0	978.0	0.25	7.35698e-3
40.06	153440.0	974.0	0.25	6.48641e-3
45.02	175880.0	969.0	0.25	5.7955e-3
50.06	201890.0	961.0	0.25	5.25449e-3
51.06	207330.0	959.4	0.25	5.17075e-3
52.12	213010.0	957.8	0.25	5.08700e-3
53.08	218210.0	956.2	0.25	5.00326e-3
54.07	223610.0	954.6	0.25	4.91951e-3
55.04	229130.0	953.0	0.25	4.83577e-3
56.12	235610.0	950.0	0.25	4.77138e-3
57.06	241460.0	947.0	0.25	4.70698e-3
58.11	248290.0	943.0	0.25	4.64259e-3
59.05	254460.0	940.0	0.25	4.57819e-3
60.09	261700.0	938.0	0.25	4.5138e-3
61.08	269040.0	935.0	0.25	4.46408e-3
62.11	276640.0	932.0	0.25	4.41435e-3
63.15	283590.0	929.0	0.25	4.36463e-3
64.05	287960.0	928.5	0.25	4.31490e-3
65.28	292940.0	928.0	0.25	4.26518e-3
70.00	311250.0	925.0	0.25	4.06861e-3
80.00	348920.0	919.0	0.25	3.757e-3
100.00	424270.0	907.0	0.25	3.05588e-3

Figure 24: Example of a material data file

2.5 Subcooling and hysteresis of the PCM material

For a lot of PCM materials the consideration of subcooling and hysteresis effects is necessary. Subcooling means that the material does not crystallize at its melting temperature but at a temperature that can be much lower. After the crystallization sets in the temperature increases until it reaches the melting temperature, at which the latent heat is set free. For some materials the temperature does not reach the melting temperature, instead the latent heat is set free at a temperature slightly lower. Both the effect and the temperature difference between this temperature and the melting temperature are referred to as hysteresis. As an example Figure 25 shows the enthalpy-temperature functions of a PCM with the subcooling $\mathrm{DT}_{\mathrm{sc}}$ and the hysteresis $\mathrm{DT}_{\mathrm{hyst}}$.

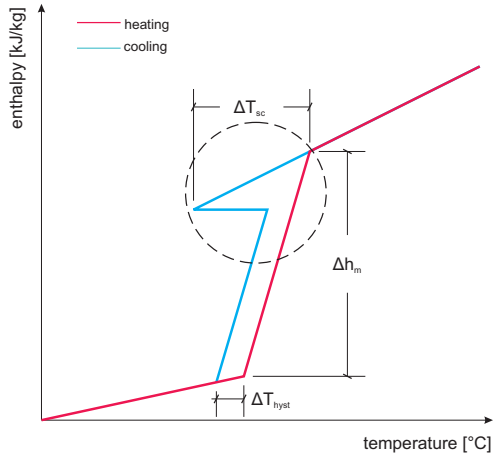

Figure 25: Example for the subcooling and hysteresis of a PCM (qualitative); the circle indicates the area magnified in Figure 26

These effects are modelled in a relatively simple way by using different enthalpy-temperature functions for heating and cooling of the material. The basic approach is shown schematically in Figure 26 and Figure 27. If the temperatures of all PCM nodes are higher than $\mathrm{T}_{\mathrm{critical2}}$ the

whole module is assumed to be fully melted. This means a transition from the heating to the cooling function, which is identical to the heating function for temperatures higher than $T_{critical2}$. Thus the temperatures of the nodes are not changing due to this transition.

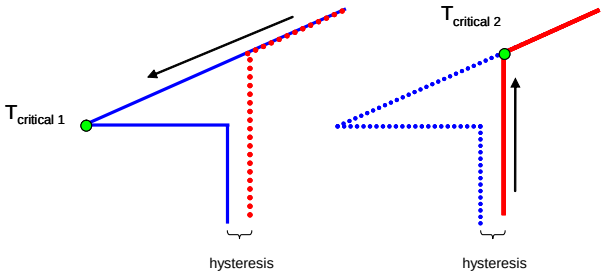

Figure 26: Critical temperatures for the transition between the enthalpy-temperature function for heating and cooling

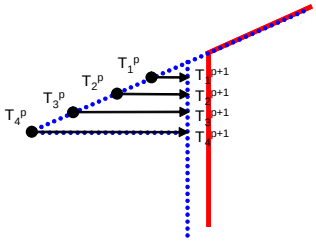

Figure 27: Transition from the cooling to the heating function (corrected by the hysteresis) from time step (p) to time step (p+1)

If the temperature of any node in the PCM module falls below $T_{critical1}$ during the cooling process, the transition from the cooling to the heating function is done. In case of a material with a hystersis a modified heating function is used (parallel shift of the phase change temperature range to lower temperatures by DT_{hyst} → compare Figure 27). Due to the transition between the enthalpy functions all PCM temperatures are increased to the temperatures with the same enthalpy on the heating function (corrected by DT_{hyst}), as it is shown in Figure 27. The transition to the original heating function is done when the energy content of the PCM increases from one time step to the next. When all temperatures exceed $T_{critical2}$ during heating the transition back to the cooling function is done.

2.6 Validation of Type 840

The storage tank model has been validated with measurements carried out at the Institute of Thermal Engineering and by measurement data provided by project partners of IEA SHC Task 32. The validations included a tank filled with a PCM slurry (charging and discharging via an internal heat exchanger and via a double port), a tank with spherical PCM modules and a tank with cylindrical PCM modules (different PCM materials). The results of this work have been published in (Puschnig et al., 2005) and (Schranzhofer et al., 2006). Concerning the results obtained with water tanks (Solé, 2006) the model was compared to a well validated water storage model (Drück, 2000).

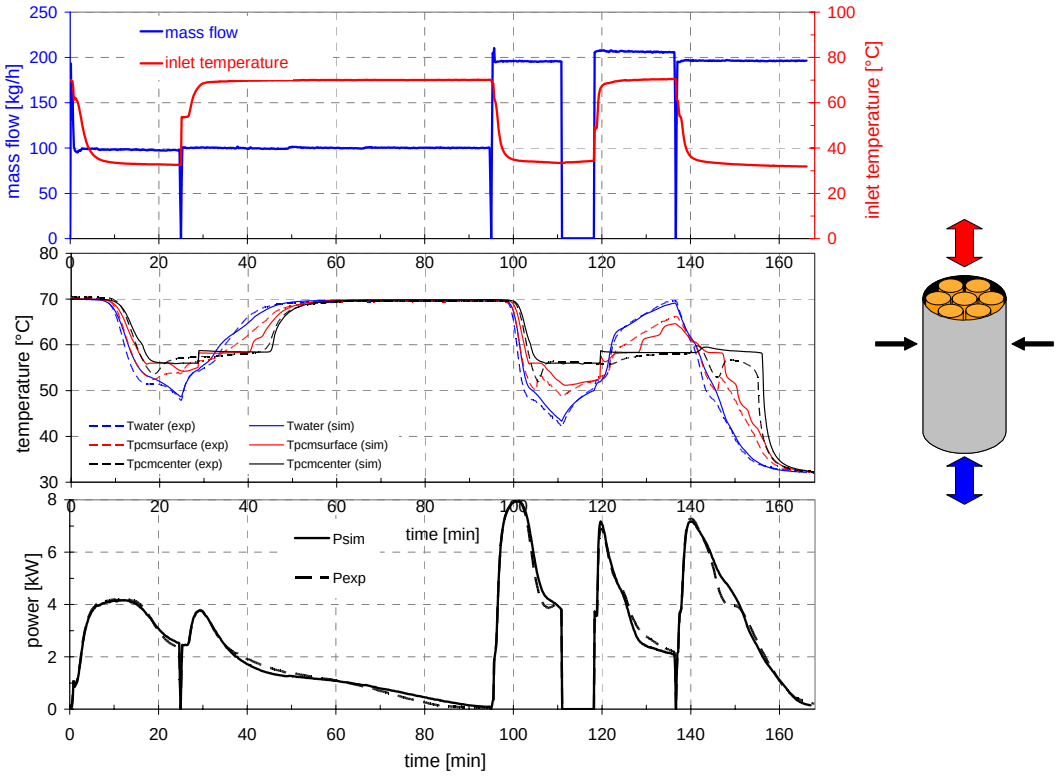

Figure 28: Comparison between measurement and simulation for an experiment with alternating charging and discharging of an experimental tank; mass flow and inlet temperature (top), measured and simulated evolution of the temperatures in the tank at the position indicated by arrows (centre), charging and discharging power (bottom)

As an example Figure 28 shows a comparison between a measurement and a simulation, in which an experimental tank with cylindrical modules, filled with Sodium Acetate Trihydrate + Graphite, is alternately charged and discharged. In the upper part of the figure the measured mass flows and the inlet temperatures are shown, which are also used as the inputs for the model. In the centre the measured and calculated temperatures at the position indicated by arrows in the figure are plotted. The bottom part of the figure shows the evolution of the measured and simulated charging and discharging powers (as absolute values). The agreement of the calculated and measured temperatures is quite good, although there is still room for improvement. However, for the correct simulation of the interaction of the tank with the rest of the system the resulting outlet temperatures and charging/discharging powers are more important. In this regard the results achieved with the model satisfy the requirements.

2.7 Acknowledgements

The European Commission is thanked for funding the work undertaken as part of the project PAMELA ENK6-CT2001-00507.

The Austrian ministry BMVIT is thanked for the financing of the projects:

- „Fortschrittliche Wärmespeicher zur Erhöhung von solarem Deckungsgrad und Kesselnutzungsgrad sowie Emissionsverringerung durch verringertes Takten, Projekt zum IEA-SHC Task 32“ Proj. Nr. 807807

- „N-GL. IEA SHC; Task Solarthermische Anlagen mit fortschrittlicher Speicher¬technologie für Niedrigenergiegebäude“ Proj. Nr. 805790

We also want to thank the industrial partners “BASF” and “SGL Carbon” for their support and the supply with PCM materials.

2.8 References

Claußen T. (1993)
Entwicklung und experimentelle Verifizierung eines dynamischen Latentwärmespeichermodells; Diplomarbeit am Studiengang Diplom-Physik, Universität Oldenburg

Drück H. (2000)
Multiport store-model for Trnsys. Stratified fluid storage tank with four internal heat exchangers, ten connections for direct charge and discharge and an internal electrical heater. Type 140, version 1.99B. November 2000.

European-Project PAMELA (2004)
Phase Change Material Slurries and Their Commercial Application (PAMELA), European project in the 5th framework, 2001-2004, Project number ENK6-CT-2001-00507

Heinz A., Streicher W., Wallner G., Schobermayr H., Puschnig P., Schranzhofer H., Eisl G., Heimrath R. (2006)
Endbericht zum Projekt “Fortschrittliche Wärmespeicher zur Erhöhung von solarem Deckungsgrad und Kesselnutzungsgrad sowie Emissionsverringerung durch verringertes Takten”, Projekt im Rahmen der Programmlinie Energiesysteme der Zukunft, Impulsprogramm Nachhaltig Wirtschaften

Puschnig P., Heinz A., Streicher W. (2005)
Trnsys simulation model for an energy storage for PCM slurries and/or PCM modules, 2nd Phase Change Material and Slurry Scientific Conference & Business Forum, Yverdon-les-Bains, Switzerland, June 15-17

Schranzhofer H., Heinz A. Puschnig P., Streicher W. (2006)
Validation of a TRNSYS simulation model for PCM energy storages and PCM wall construction elements, Ecostock Conference, 31th May – 2nd June 2006, Stockton College, Pomona, USA

Solé C. (2006)
Report on annual simulations with a combisystem with PCM modules in a solar system with TRNSYS to optimize the PCM configuration inside the storage tank; Internal report, Institute of Thermal Engineering, Graz Technical University

Trnsys 16 (2005)
TRNSYS 16, A Transient System Simulation Program, V 16.0.038, Solar Energy Lab, University of Wisconsin - Madison, USA, 2005.

VDI Wärmeatlas (1997)
Wärmeübergang und Strömung in Verfahrenstechnik und Chemie, 8. Auflage, Springer Verlag

Visser H. (1986)
Energy Storage in Phase Change Materials, Development of a component model compatible with the TRNSYS transient simulation program; Department of Applied Physics, Delft University of Technology

2.9 Annex: Parameters, Inputs and Outputs of the model

List of parameters

Nr.	Description	Unit [lower limit; upper limit]
1	Volume of storage	m^3 [0;100]
2	Height of storage	m [0;10]
3	Heat loss rate	W/K [0;1000]
4	Fluid number of storage fluid	- [0;3]
5	Number of nodes	- [1;200]
6	Initial temperature of store	C [0;100]
7	Position of aux. heater (top)	- [0;1]
8	Position of aux. heater (bottom)	- [0;1]
9	Effective vertical thermalt conductivity	W/m.K [0;100]
10	Logical unit fluid number 1	- [30;99]
11	Logical unit fluid number 2	- [30;99]
12	Logical unit fluid number 3	- [30;99]
13	Number of temperature sensors	- [1;10]
14	Position of top sensor	- [0;1]
15	Position of bottom sensor	- [0;1]
16	DP1: type	- [0;1]
17	DP1: fluid number	- [0;3]
18	DP1: inlet height	- [0;1]
19	DP1: outlet height	- [0;1]
20	DP1: height of temperature sensor	- [0;1]
21	DP1: Length of HX pipe	m [0;200]
22	DP1: Inner diameter of HX pipe	mm [0;100]
23	DP1: Outer diamter of HX pipe	mm [0;100]
24	DP1: Therm. Cond. of pipe wall	W/m.K [0;5000]
25	DP1: Heat transfer per pipe length	W/m.K [-50;200.0]
26	DP2: type	- [0;1]

27	DP2: fluid number	- [0;3]
28	DP2: inlet height	- [0;1]
29	DP2: outlet height	- [0;1]
30	DP2: height of temperature sensor	- [0;1]
31	DP2: Length of HX pipe	m [0;200]
32	DP2: Inner diameter of HX pipe	mm [0;100]
33	DP2: Outer diamter of HX pipe	mm [0;100]
34	DP2: Therm. Cond. of pipe wall	W/m.K [0;5000]
35	DP2: Heat transfer per pipe length	W/m.K [-50;200]
36	DP3: type	- [0;1]
37	DP3: fluid number	- [0;3]
38	DP3: inlet height	- [0;1]
39	DP3: outlet height	- [0;1]
40	DP3: height of temperature sensor	- [0;1]
41	DP3: Length of HX pipe	m [0;200]
42	DP3: Inner diameter of HX pipe	mm [0;100]
43	DP3: Outer diamter of HX pipe	mm [0;100]
44	DP3: Therm. Cond. of pipe wall	W/m.K [0;5000]
45	DP3: Heat transfer per pipe length	W/m.K [-50;200]
46	DP4: type	- [0;1]
47	DP4: fluid number	- [0;3]
48	DP4: inlet height	- [0;1]
49	DP4: outlet height	- [0;1]
50	DP4: height of temperature sensor	- [0;1]
51	DP4: Length of HX pipe	m [0;200]
52	DP4: Inner diameter of HX pipe	mm [0;100]
53	DP4: Outer diamter of HX pipe	mm [0;100]
54	DP4: Therm. Cond. of pipe wall	W/m.K [0;5000]
55	DP4: Heat transfer per pipe length	W/m.K [-50;200]
56	DP5: type	- [0;1]
57	DP5: fluid number	- [0;3]
58	DP5: inlet height	- [0;1]
59	DP5: outlet height	- [0;1]
60	DP5: height of temperature sensor	- [0;1]
61	DP5: Length of HX pipe	m [0;200]
62	DP5: Inner diameter of HX pipe	mm [0;100]
63	DP5: Outer diamter of HX pipe	mm [0;100]
64	DP5: Therm. Cond. of pipe wall	W/m.K [0;5000]
65	DP5: Heat transfer per pipe length	W/m.K [-50;200]
66	PCM1: number of modules	- [0;+Inf]
67	PCM1: fluid number	- [0;3]
68	PCM1: geometry 0 = cyl, 1 = sph	- [0;1]
69	PCM1: Inner diameter (cyl)	mm [0;500]
70	PCM1: Outer diameter	mm [0;500]
71	PCM1: Number of radial nodes	- [1;20]
72	PCM1: position in tank (top)	- [0;1]
73	PCM1: position in tank (bottom)	- [0;1]
74	PCM1: thickness container	mm [0;10]
75	PCM1: therm. cond. container	W/m.K [0;5000]
76	PCM1: cp of container material	J/kgK
77	PCM1: mass density of container material	kg/m^3

78	PCM2: number of modules	- [0;+Inf]
79	PCM2: fluid number	- [0;3]
80	PCM2: geometry 0 = cyl, 1 = sph	- [0;1]
81	PCM2: Inner diameter (cyl)	mm [0;500]
82	PCM2: Outer diameter	mm [0;500]
83	PCM2: Number of radial nodes	- [1;20]
84	PCM2: position in tank (top)	- [0;1]
85	PCM2: position in tank (bottom)	- [0;1]
86	PCM2: thickness container	mm [0;10]
87	PCM2: therm. cond. container	W/m.K [0;5000]
88	PCM2: cp of container material	J/kgK
89	PCM2: mass density of container material	kg/m^3
90	PCM3: number of modules	- [0;+Inf]
91	PCM3: fluid number	- [0;3]
92	PCM3: geometry 0 = cyl, 1 = sph	- [0;1]
93	PCM3: Inner diameter (cyl)	mm [0;500]
94	PCM3: Outer diameter	mm [0;500]
95	PCM3: Number of radial nodes	- [1;20]
96	PCM3: position in tank (top)	- [0;1]
97	PCM3: position in tank (bottom)	- [0;1]
98	PCM3: thickness container	mm [0;10]
99	PCM3: therm. cond. container	W/m.K [0;5000]
10 0	PCM3: cp of container material	J/kgK
10 1	PCM3: mass density of container material	kg/m^3

List of inputs

Nr.	Description	Unit [lower limit; upper limit]
1	inlet temperature 1	C [-Inf;+Inf]
2	inlet mass flow rate 1	kg/hr [-Inf;+Inf]
3	inlet temperature 2	C [-Inf;+Inf]
4	inlet mass flow rate 2	kg/hr [-Inf;+Inf]
5	inlet temperature 3	C [-Inf;+Inf]
6	inlet mass flow rate 3	kg/hr [-Inf;+Inf]
7	inlet temperature 4	C [-Inf;+Inf]
8	inlet mass flow rate 4	kg/hr [-Inf;+Inf]
9	inlet temperature 5	C [-Inf;+Inf]
10	inlet mass flow rate 5	kg/hr [-Inf;+Inf]
11	Ambient temperature	C [-Inf;+Inf]
12	Auxiliary heater power	W [-Inf;+Inf]

List of outputs

Nr.	Description	Unit [lower limit; upper limit]
1	Outlet temperature 1	C [-Inf;+Inf]
2	Outlet mass flow rate 1	kg/hr [-Inf;+Inf]
3	Outlet temperature 2	C [-Inf;+Inf]
4	Outlet mass flow rate 2	kg/hr [-Inf;+Inf]
5	Outlet temperature 3	C [-Inf;+Inf]
6	Outlet mass flow rate 3	kg/hr [-Inf;+Inf]
7	Outlet temperature 4	C [-Inf;+Inf]

8	Outlet mass flow rate 4	kg/hr [-Inf;+Inf]
9	Outlet temperature 5	C [-Inf;+Inf]
10	Outlet mass flow rate 5	kg/hr [-Inf;+Inf]
11	Total energy of store	kWh [-Inf;+Inf]
12	Energy of storage fluid	kWh [-Inf;+Inf]
13	Energy in internal HX1	kWh [-Inf;+Inf]
14	Energy in internal HX2	kWh [-Inf;+Inf]
15	Energy in internal HX3	kWh [-Inf;+Inf]
16	Energy in internal HX4	kWh [-Inf;+Inf]
17	Energy in internal HX5	kWh [-Inf;+Inf]
18	Energy in PCM module1	kWh [-Inf;+Inf]
19	Energy in PCM module2	kWh [-Inf;+Inf]
20	Energy in PCM module3	kWh [-Inf;+Inf]
21	Energy in PCM container1	kWh [-Inf;+Inf]
22	Energy in PCM container2	kWh [-Inf;+Inf]
23	Energy in PCM container3	kWh [-Inf;+Inf]
24	Power through double port1	kW [-Inf;+Inf]
25	Power through double port2	kW [-Inf;+Inf]
26	Power through double port3	kW [-Inf;+Inf]
27	Power through double port4	kW [-Inf;+Inf]
28	Power through double port5	kW [-Inf;+Inf]
29	Heat loss rate to ambient	kW [-Inf;+Inf]
30	Power by auxliary heater	kW [-Inf;+Inf]
31	Heat transfer rate to PCM1	kW [-Inf;+Inf]
32	Heat transfer rate to PCM2	kW [-Inf;+Inf]
33	Heat transfer rate to PCM3	kW [-Inf;+Inf]
34	Temperature sensor 1	C [-Inf;+Inf]
35	Temperature sensor 2	C [-Inf;+Inf]
36	Temperature sensor 3	C [-Inf;+Inf]
37	Temperature sensor 4	C [-Inf;+Inf]
38	Temperature sensor 5	C [-Inf;+Inf]
39	Fluid temperature 1 bottom	C [-Inf;+Inf]
40	Fluid temperature 2	C [-Inf;+Inf]
41	Fluid temperature 3	C [-Inf;+Inf]
42	Fluid temperature 4	C [-Inf;+Inf]
43	Fluid temperature 5	C [-Inf;+Inf]
44	Fluid temperature 6	C [-Inf;+Inf]
45	Fluid temperature 7	C [-Inf;+Inf]
46	Fluid temperature 8	C [-Inf;+Inf]
47	Fluid temperature 9	C [-Inf;+Inf]
48	Fluid temperature 10 top	C [-Inf;+Inf]
49	PCM temperature 1 bottom	C [-Inf;+Inf]
50	PCM temperature 2	C [-Inf;+Inf]
51	PCM temperature 3	C [-Inf;+Inf]
52	PCM temperature 4	C [-Inf;+Inf]
53	PCM temperature 5	C [-Inf;+Inf]
54	PCM temperature 6	C [-Inf;+Inf]
55	PCM temperature 7	C [-Inf;+Inf]
56	PCM temperature 8	C [-Inf;+Inf]
57	PCM temperature 9	C [-Inf;+Inf]
58	PCM temperature 10 top	C [-Inf;+Inf]

3 TYPE 841 - MODEL FOR THE TRANSIENT SIMULATION OF BULK PCM TANKS WITH AN IMMERSED WATER-TO-AIR HEAT EXCHANGER

Andreas Heinz, Institute of Thermal Engineering, Graz University of Technology, Austria

3.1 Introduction

At the Institute of Thermal Engineering the approach to use a bulk PCM storage tank with an immersed water-to-air heat exchanger was investigated. This approach is favorable compared to a water tank with integrated PCM modules for small short term storages that require high specific charging/discharging powers. For the simulation of such tanks Type 840 (Puschnig, 2004)) can not be used, as it is limited to PCM-modules of different geometries that are integrated into a tank. In order to enable a calculation of the heat transfer processes occurring via the finned tubes of a water-to-air heat exchanger the development of a second model was necessary. The model is called Type 841 and was implemented into TRNSYS 16.

Water-to-air heat exchangers are typically built as fin-tube heat exchangers with circular tubes and continuous plate fins. A schematic of a possible design of such a heat exchanger is shown in Figure 29. Typically there are several parallel tube coils, consisting of a number of tubes that are connected in series. In the case shown in the picture there are three coils, each consisting of 8 tubes in series. As shown in Figure 30 the arrangement of the tubes in the heat exchanger can be either aligned or staggered. The model has been formulated to enable a calculation of both kinds of tube arrangements. However, the description that is given here is related to aligned tubes.

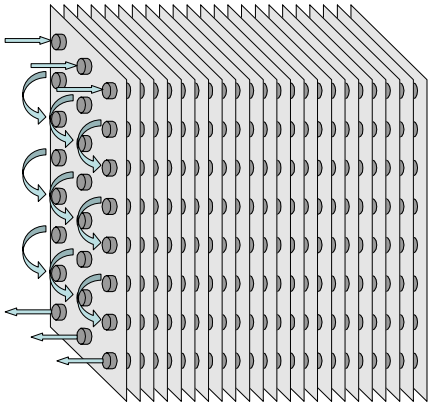

Figure 29: Water-to-air heat exchanger consisting of tubes and fins

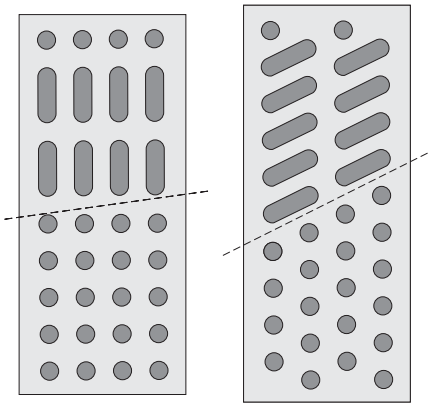

Figure 30: Tube arrangement: aligned (left) and staggered (right); the upper part of the figure shows the connections between the pipes in series, the lower part shows a cross section of the heat exchanger

In order to promote the heat transfer between the heat carrier fluid in the tubes and the air flow on the outside a large number of fin plates are attached to the tubes. In the application shown here, where the heat exchanger is used in a PCM tank, the spacings between the fins

are filled with the PCM material, the fins thereby increasing the heat transfer from the PCM to the heat carrier fluid and vice versa.

The PCM storage tank is now assumed to consist of the heat exchanger and a rectangular casing that is built around it. The PCM is filled into the spaces between the fins of the heat exchanger.

The notations of the dimensions of the heat exchanger tubes and the fins that are needed for the calculations in the model are shown in Figure 31. The model was validated against the measurements obtained with a storage tank of this type that was built at the Institute o Thermal Engineering. The relevant data and dimensions of the used heat exchanger are given in Table 6 on page 63.

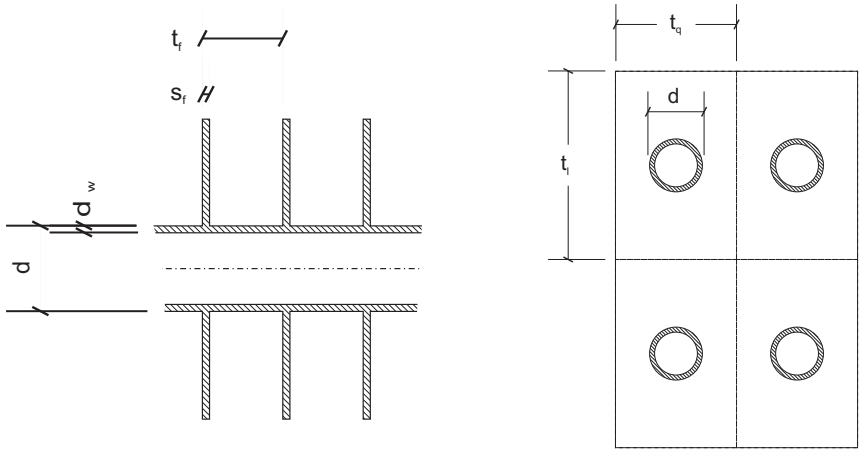

Figure 31: Left: longitudinal section of a finned tube and its dimensions ; right: cross section of four aligned tubes with its dimensions

3.2 Basic assumptions and simplifications

The model is based on finite differences in the explicit formulation. The modeling of the phase change from solid to liquid is based on the enthalpy method (Claußen, 1993) (Visser, 1986). The heat exchanger is subdivided into nodes, whereby each node represents a certain region and its temperature is a measure of the average temperature of this region. As shown in Figure 32 the structure of the nodal network is chosen in the following way:

The tank volume is subdivided into nodes of equal size, later on referred to as Storage-nodes, each consisting of a tube section and the surrounding fin- and PCM-material. Thus every node has the width tq and the height tl, the length depends on the chosen number of nodes. The volume of a storage node does not include the volume of the heat carrier fluid in the tube. The thermal capacities of all the materials within the node (PCM, fin, tube) are considered, but as they are all together referred to as one single node, they are assumed to have the same temperature. Physically this is not correct, because of the three-dimensional heat transfer processes and the resulting temperature gradients between tube, fins and PCM. However, as the distances between the tubes of such heat exchangers are typically

quite small, this simplification is made. For the heat carrier fluid in the heat exchanger tubes separate nodes are defined, with the diameter d and the same length as the storage nodes.

For each node an energy conservation equation is formulated in chapter 3.3. The evolution of the temperatures with time is calculated with the explicit method, i.e. the enthalpies in the new time step (p+1) are calculated out of the temperatures in the previous time step (p) (Incropera, 2002). Heat transfer in the PCM is only calculated by means of conduction. Convection, which occurs when the PCM is in the liquid state, is not considered. This simplification is made because the space between the fins is very small and the convection effects will be very low anyhow.

In case of several parallel tube coils, like in Figure 29, only one coil is calculated, assuming that the behavior of all parallel coils is the same. The energy losses of the tank to the ambient are evenly distributed over all nodes of the tank.

As depicted in Figure 32 the tubes in series are connected by pipe bends, which create a certain volume inside of the tank, which is not reached by the fins of the heat exchanger. In this regions heat transfer will be limited by the thermal conductivity of the PCM and convective heat transfer in the liquid state. The heat transfer effects in these regions are also not considered in the model. The PCM mass, which is contained in these regions, is as a simplification added to the PCM mass contained in the storage nodes. As the limited heat transfer in these regions is not considered, the model may deliver slightly better results compared to reality (concerning the discharge power) for tanks with large spaces between the heat exchanger and the walls of the casing.

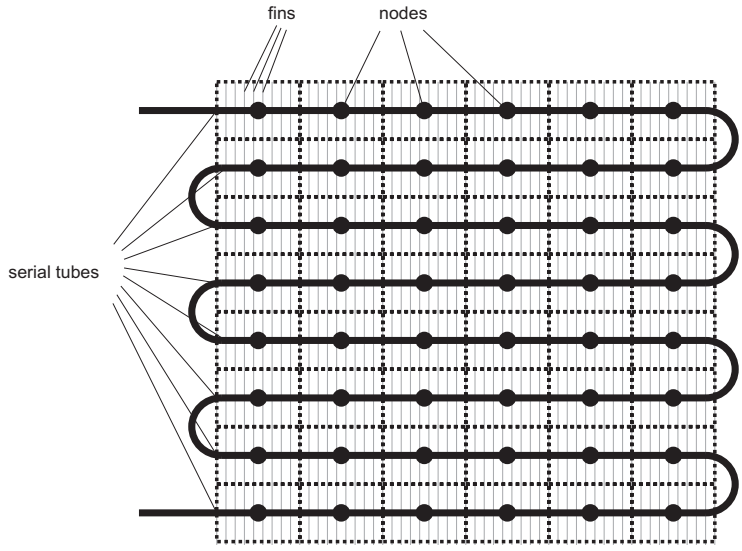

Figure 32: Common structure of the nodal network of the model

3.3 Governing equations

The detailed structure of the nodal network used as a basis for the governing equations of the model is depicted in Figure 33. The indices (m) and (n) denote the location of the storage

nodes in the directions m (the direction of the tubes) and n (the direction perpendicular to the tubes).

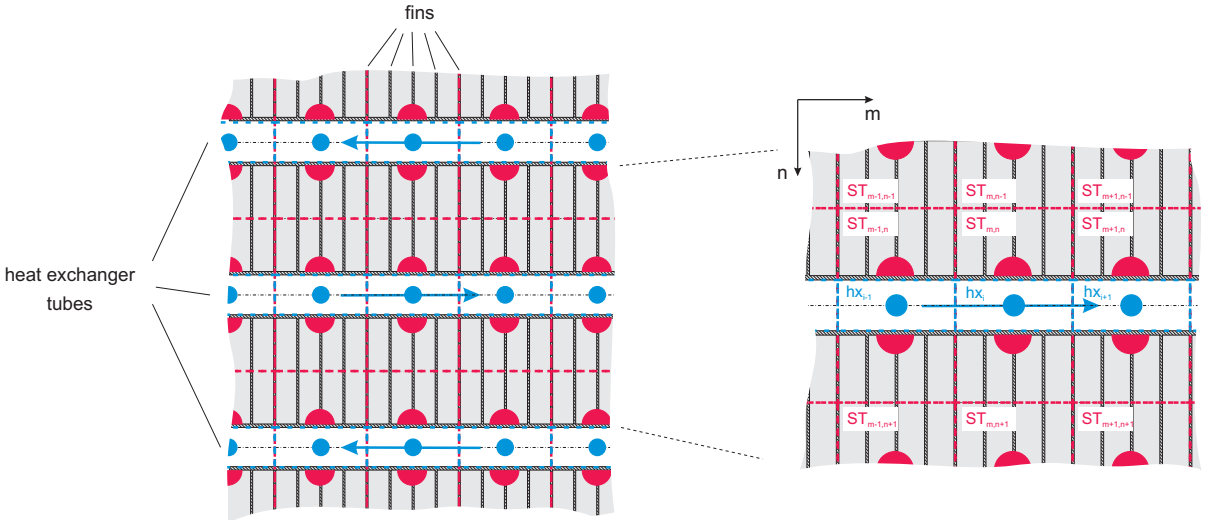

Figure 33: Detailed structure of the nodal network

3.3.1 Heat exchanger nodes

As the heat exchanger tubes typically have a quite small diameter, the flow velocities are rather high (depending on the current mass flow rate $\dot{m}_{hx}$). If a transient calculation with the explicit approach would be used in this case, very small time steps would be required in order to ensure numerical stability. An evaluation of the maximum size of the time step is shown in chapter 3.5. In order to avoid long simulation times, it was decided to perform a steady-state calculation of the temperatures of the heat carrier fluid in every time step. Using this approach the transient behavior and the thermal capacity of the heat carrier fluid, which is only a small part of the total capacity of the tank (small water content in the tubes compared to the total volume of the tank, high storage capacity of PCM compared to water), is not accounted for.

The nodes of the heat carrier fluid are characterized by their temperature T_{hx_i}, whereby the location of the node in flow direction is designated by the index (i). The energy conservation equation for one node is expressed as

$$\dot{m}_{hx} c_{p_{hx}} \left(T_{hx_{i-1}} - T_{hx_i}\right) = UA_{tot} n_{el} \left(T_{hx_{i-1}} - T_{ST}\right) \qquad (14)$$

where T_{ST} is the temperature of the adjoining storage node and A_{tot} is the surface area of one element, consisting of the fin surface A_f (both sides of the fin) and the surface of the tube segment between two fins A_{tube} (see Equation (15)). n_{el} is the number of such elements in one storage node (e.g. 4 in Figure 33).

$$A_{tot} = A_f + A_{tube} = (2t_q t_l - d^2 \frac{p}{2}) + dp(t_f - s_f) \qquad (15)$$

U is the overall heat transfer coefficient from the heat carrier fluid to the PCM (based on the heat transfer surface facing the PCM). The calculation of U is explained in chapter 3.4. The temperatures of the heat exchanger nodes can now be calculated:

$$T_{hx_i} = T_{hx_{i-1}} - \frac{UA_{tot} n_{el} (T_{hx_{i-1}} - T_{ST})}{\dot{m}_{hx} c_{p_{hx}}} \quad (16)$$

Starting the calculation with the known inlet temperature of the heat exchanger and progressing in flow direction, the temperature of node (i) is calculated out of the temperature of the previous heat exchanger node (i-1) and the temperature of the adjoining storage node T_{ST}.

3.3.2 Storage nodes

According to the enthalpy method the storage nodes are characterized by their enthalpy h_{ST}. The energy conservation equation of a storage node has the form

$$m_{ST} \frac{h^{p+1}_{ST_{m,n}} - h^{p}_{ST_{m,n}}}{\Delta t} = \dot{Q}^{p}_{hx} + \dot{Q}^{p}_{cond,m} + \dot{Q}^{p}_{cond,n} + \dot{Q}^{p}_{loss} \quad (17)$$

where m_{ST} is the mass of a storage node and Δt the used time step from the time (p) to time (p+1). The left side of the equation describes the evolution of the enthalpy of the node (m,n) with time, the right side expresses the heat flows in and out of the respective node. (hx) denotes the heat exchange with the heat carrier fluid in the tube, (cond,m) and (cond,n) the conduction to adjoining storage nodes in the direction m and n, and (loss) the energy losses to the ambient. Rearranging equation (17) the enthalpy of node (m,n) in the new time step is computed with:

$$h^{p+1}_{ST_{m,n}} = h^{p}_{ST_{m,n}} + (\dot{Q}^{p}_{hx} + \dot{Q}^{p}_{cond,m} + \dot{Q}^{p}_{cond,n} + \dot{Q}^{p}_{loss}) \frac{\Delta t}{m_{ST}} \quad (18)$$

The temperatures of the storage nodes are calculated out of the enthalpies according to the enthalpy-temperature functions described in section 3.6.

Heat flow from the heat exchanger

The heat exchange $\dot{Q}_{hx}$ between the heat exchanger tube and the storage node (m,n) is calculated according to Equation (19)

$$\dot{Q}^{p}_{hx} = UA_{tot} n_{el} (T^{p}_{hx} - T^{p}_{ST_{m,n}}) \quad (19)$$

where T^{p}_{hx} is the temperature of the adjoining heat exchanger node.

Conduction between adjoining storage nodes

The heat transfer by conduction between the storage nodes is considered both in the direction m and n. During the charging or discharging processes the conduction heat flow between the storage nodes is negligible compared to the heat flow between the storage nodes and the heat exchanger. However, these heat flows have to be accounted for, as they cause a diminishing of temperature stratifications in the tank, especially in times when the heat exchanger is not operated.

The calculation is performed according to Equation (20) and (21), where A_f is the surface area of a fin and λ_m and λ_n are the average thermal conductivities in the directions m and n. The dimensions t_f, s_f, t_q, t_l can be seen in Figure 31.

$$\dot{Q}^p_{cond,m} = \frac{\lambda_m}{n_{el} t_f} \frac{A_f}{2} (T^p_{ST_{m+1,n}} + T^p_{ST_{m-1,n}} - 2 T^p_{ST_{m,n}}) \tag{20}$$

$$\dot{Q}^p_{cond,n} = \frac{\lambda_n}{t_l} (t_q n_{el} t_f) (T^p_{ST_{m,n+1}} + T^p_{ST_{m,n-1}} - 2 T^p_{ST_{m,n}}) \tag{21}$$

The thermal conductivity in the direction m is calculated by adding the thermal resistances of the fin- and PCM-layer according to Equation (22).

$$\lambda_m = \frac{t_f}{\frac{t_f - s_f}{\lambda_{PCM}} + \frac{s_f}{\lambda_f}} \tag{22}$$

λ_n is calculated as an average value out of the conductivity of the PCM λ_{PCM} and the fin λ_f:

$$\lambda_n = (\lambda_{PCM}(t_f - s_f) + \lambda_f s_f) \frac{1}{t_f} \tag{23}$$

Losses to the ambient

The losses to the ambient are computed according to Equation (24), using the losses of the whole tank per temperature difference to the ambient $(UA)_{loss}$, the number of nodes in one tube coil n_{nodes_t} and the number of parallel tube coils $n_{tubes_{par}}$.

$$\dot{Q}^p_{loss} = \frac{(UA)_{loss}}{n_{nodes_t} n_{tubes_{par}}} (T^p_{amb} - T^p_{ST_{m,n}}) \tag{24}$$

3.4 Calculation of the heat transfer from the finned tubes

The calculation of the heat transfer from the finned tubes is performed according to VDI Wärmeatlas (1997). The overall heat transfer coefficient, based on the heat transfer surface facing the PCM and the temperature difference between the heat carrier fluid and the PCM, is calculated as follows:

$$\frac{1}{U} = \frac{1}{a_s} + \frac{A_{tot}}{A_{tube,i}}\left(\frac{1}{a_i} + \frac{d_w}{l_t}\right) \tag{25}$$

where a_i is the convective heat transfer coefficient on the inside surface of the heat exchanger tube $A_{tube,i}$, which is calculated out of empirical correlations for laminar and turbulent flow in circular tubes (VDI Wärmeatlas, 1997). l_t is the thermal conductivity of the heat exchanger tubes. a_s is an effective heat transfer coefficient, which is calculated out of the heat transfer coefficient on the fin and pipe surface a_f and the fin efficiency h_f as follows:

$$a_s = a_f\left[1 - (1 - h_f)\frac{A_f}{A_{tot}}\right] \tag{26}$$

In this application the medium on the fin surface of the heat exchanger is not moving air but the PCM. This means that there will be no movement of the medium, except because of natural convection effects. As the cavities between the fins are quite narrow, there should be only very low convection, or no convection at all when the PCM is in the solid state. Thus the heat transfer coefficient a_f is defined according to Equation (27) by the thermal conductivity of the PCM l_{PCM} and half of the distance between two fins.

$$a_f = \frac{2l_{PCM}}{t_f - s_f} \tag{27}$$

The fin efficiency is calculated with

$$h_f = \frac{\tanh X}{X} \tag{28}$$

with

$$X = j\,\frac{d}{2}\sqrt{\frac{2a_f}{l_f s_f}} \tag{29}$$

For rectangular fins j is

$$j = (j' - 1)(1 + 0.35 \ln j') \tag{30}$$

According to (VDI Wärmeatlas, 1997) the calculation of j' is done depending on the fin geometry (t_q, t_l, tube diameter d, aligned or staggered tube arrangement) and shall not be described in detail.

3.5 Numerical stability and internal time step

An undesirable feature of the here used explicit method is that it is not unconditionally stable. In a transient problem the solution for the nodal temperatures should continuously approach final (steady state) values with increasing time. However, with the explicit method this solution may be characterized by numerically induced oscillations, which are physically impossible. The oscillations may become unstable, causing the solution to diverge from the actual steady-state conditions. To prevent such erroneous results, the prescribed value of the time step Δt must be maintained below a certain limit, which depends on certain parameters of the system. This dependence is termed a stability criterion. For the problem of interest in this work, the criterion can be determined by requiring that the coefficient associated with the temperature in the node of interest at the previous time is greater than or equal to zero. In general, this is done by collecting all terms involving T^p to obtain the form of the coefficient. This result is then used to obtain a limiting relation, from which the maximum allowable value of Δt can be determined (Incropera, 2002).

Heat exchanger nodes

As mentioned before it was decided to calculate the temperature distribution in the heat exchanger tubes only as a steady state for each time step. This is because a transient simulation would require very small time steps. This shall be demonstrated here.

The energy conservation equation for a heat exchanger node in its transient form is

$$m_{hx} c_{p_{hx}} \frac{T_{hx_i}^{p+1} - T_{hx_i}^{p}}{\Delta t} = \dot{m}_{hx} c_{p_{hx}} \left(T_{hx_{i-1}}^{p} - T_{hx_i}^{p}\right) + UA_{tot} n_{el} \left(T_{ST}^{p} - T_{hx_i}^{p}\right) \tag{31}$$

where m_{hx} is the mass of one heat exchanger node and $c_{p_{hx}}$ is the specific heat capacity of the heat carrier fluid. By collecting all terms involving $T_{hx_i}^{p}$ the coefficient associated with the node of interest at the previous time is obtained. The stability criterion is, that this coefficient is greater than or equal to zero:

$$m_{hx} c_{p_{hx}} \frac{1}{\Delta t} - \dot{m}_{hx} c_{p_{hx}} - UA_{tot} n_{el} \geq 0 \tag{32}$$

The maximum value of the time step Δt can now be determined with

$$\Delta t \leq \frac{m_{hx} c_{p_{hx}}}{\dot{m}_{hx} c_{p_{hx}} + UA_{tot} n_{el}} \tag{33}$$

It can be concluded that the maximum time step increases with increasing thermal capacity of the node and thus with the size of the nodes and decreases with increasing heat flows in or out of the node.

Using the data of the experimental tank that was built at the Institute of Thermal Engineering with a number of nodes in one tube coil n_{nodes_t} of 100 and a mass flow rate of 500 kg/h, the maximum allowable value of Δt is 0.19 seconds. In TRNSYS a low time step like this would lead to very long simulation times. This is why a steady state approach is used.

Storage nodes

Using the energy conservation equation for a storage node (17) with all heat flows in and out of the node (19), (20), (21) and (24) the form of the stability criterion is

$$m_{ST} c_{p_{ST}} \frac{1}{\Delta t} - UA_{tot} n_{el} - \frac{l_m}{n_{el} t_f} A_f - \frac{2 l_n}{t_l} t_q n_{el} t_f - \frac{(UA)_{loss}}{n_{nodes_t} n_{tubes_{par}}} \geq 0 \tag{34}$$

In this equation $c_{p_{ST}} T_{ST}$ is used instead of h_{ST}, as the coefficient associated with T_{ST} is needed for the calculation. The maximum value of the time step Δt is determined with

$$\Delta t \leq \frac{m_{ST} c_{p_{ST}}}{UA_{tot} n_{el} + \frac{l_m}{n_{el} t_f} A_f + \frac{2 l_n}{t_l} t_q n_{el} t_f + \frac{(UA)_{loss}}{n_{nodes_t} n_{tubes_{par}}}} \tag{35}$$

For $c_{p_{ST}}$ the smaller out of the two values for the solid and the liquid state is used, as this one is crucial for the size of the time step. Depending on the size of the nodes and the heat flows the maximum time step can be several seconds or up to more than one minute.

The model was developed to be used in the simulation environment TRNSYS which is calculating with a certain time step Δt_{TRNSYS}. If this time step is higher than the maximum allowed time step of the model, problems concerning the numerical stability would arise. One solution would be to reduce the TRNSYS time step to a lower value. This approach can have the disadvantage of much higher simulation times, as all models in the TRNSYS program have to use this smaller time step. Therefore an internal time step was implemented into the model, which is calculated according to equation (35), and is then reduced to a value that fulfils $\Delta t_{TRNSYS} = N_{int} \Delta t$, where N_{int} is the integer number of internal time steps within one TRNSYS time step.

3.6 Implementation of the thermal properties of the PCM material

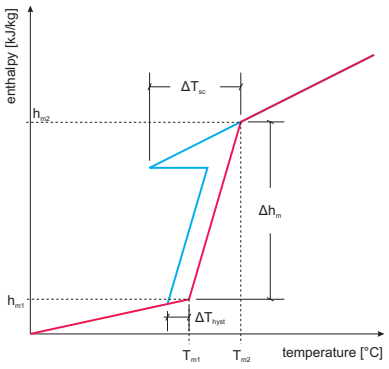

Figure 34: Enthalpy-temperature-

The new enthalpies of the storage nodes are calculated in every time step according to the equations in chapter 3.3.2. The temperatures, which are needed to calculate the enthalpies in the next time step, are then determined using enthalpy-temperature functions that are calculated out of the thermal properties of the materials provided by the user. Other than in Type 840 the thermal properties are not implemented via ASCII data files, but with a more simple approach:

As shown in Figure 34, three linear functions for the solid, liquid and phase change region are used to describe the enthalpy-temperature relation of the PCM material. For the solid and for the liquid state of the PCM a constant c_p is assumed. The phase change region is defined by the temperature range $T_{m2} - T_{m1}$ and the latent heat Dh_m. For PCMs with a wide melting range and a c_p that varies strongly with temperature inside of this range, this approach might not be sufficient. For salt hydrates and for paraffins that show a small melting range it should be detailed enough. The subcooling and hysteresis of the PCM material can be considered by providing the temperature differences DT_{sc} and DT_{hyst}.

As mentioned before, all materials contained in one storage node are calculated as one capacity. Therefore the average specific heat capacities of the storage nodes for the liquid and solid state of the PCM are calculated out of the masses and heat capacities of the tube material (t), the fin material (f), the PCM material (PCM) and an additional material (add), which could be for example the storage casing.

$$c_{p_{s,ST}} = \frac{m_t c_{p_t} + m_f c_{p_f} + m_{PCM} c_{p_{s,PCM}} + m_{add} c_{p_{add}}}{m_{ST}} \tag{36}$$

$$c_{p_{l,ST}} = \frac{m_t c_{p_t} + m_f c_{p_f} + m_{PCM} c_{p_{l,PCM}} + m_{add} c_{p_{add}}}{m_{ST}} \tag{37}$$

The latent heat of the PCM material is increased by the sensible heat in the melting range $T_{m2} - T_{m1}$ and is based on the mass of one storage node m_{ST}.

$$Dh_{m_{ST}} = \left[m_{PCM} Dh_{m_{PCM}} + m_{ST} \frac{c_{p_{s,ST}} + c_{p_{l,ST}}}{2} (T_{m2} - T_{m1}) \right] \frac{1}{m_{ST}} \tag{38}$$

With $h_{m1} = c_{p_{s,ST}} T_{m1}$ and $h_{m2} = h_{m1} + Dh_{m_{ST}}$ the temperature of a storage node can be calculated out of the respective enthalpy according to the equations (39) - (41). DT_{sc} and DT_{hyst} are set to zero, if no subcooling or hysteresis is occurring in the current state of the material.

For $h_{ST} < h_{m1} - c_{p_s} DT_{hyst}$ (*solid state*):

$$T_{ST} = h_{ST} / c_{p_{s,ST}} \tag{39}$$

For $h_{ST} \geq h_{m1} - c_{p_{s,ST}} DT_{hyst}$ and $h_{ST} < h_{m2} - c_{p_{l,ST}} DT_{sc}$ (*phase change temperature range*):

$$T_{ST} = T_{m1} - DT_{hyst} + \left(h_{ST} - h_{m1} + c_{p_{s,ST}} DT_{hyst}\right) \frac{T_{m2} - T_{m1}}{Dh_{m_{ST}}} \tag{40}$$

For $h_{ST} \geq h_{m2} - c_{p_{l,ST}} DT_{sc}$ (*liquid state*):

$$T_{ST} = T_{m2} + \frac{\left(h_{ST} - h_{m2}\right)}{c_{p_{l,ST}}} \tag{41}$$

3.7 Validation of Type 841

The results of the simulations with the developed model are compared to the results of measurements that were performed with an experimental tank that was built at the Institute of Thermal Engineering. Table 6 shows the data of the heat exchanger used in the experiments and the thermal properties, which are also used as the parameters for the simulations.

The flow rates and inlet temperatures that were measured in each time step are used as inputs for the simulation. Figure 35 shows a comparison between a simulation and a measurement with water in the tank, whereby the tank is charged from 30 to 72°C with a flow rate of about 380 kg/h.

Figure 36 shows the results for charging the tank filled with Sodium Acetate Trihydrate from a temperature of 30°C to 70°C with a flow rate of 370 kg/h. The agreement of simulation and measurement for the outlet temperature and the charging power is satisfying. At the end of the charging process, at a time of approximately 60 min, the power is already at zero in the simulation, whereas there is still a small power in the measurement. This is most likely because of the regions in the tank that are not reached by the fins of the heat exchanger (the regions with the pipe bends on the sides of the tank), which are not considered in the model. The agreement of the temperatures in the PCM leaves room for improvement. However, the more important result is the outlet temperature of the tank, which is crucial for the correct interaction with the rest of the system.

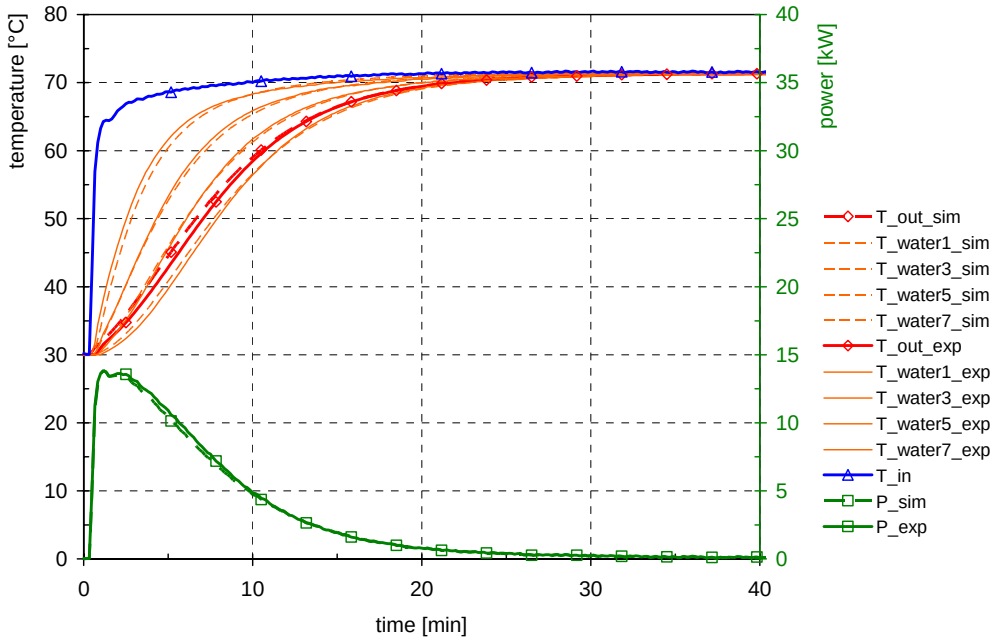

Figure 35: Comparison between simulation and measurement for charging the tank (filled with water) with a flow rate of 380 kg/h, inlet temperature 72°C; evolution of the outlet temperature, the PCM temperatures and the charging power

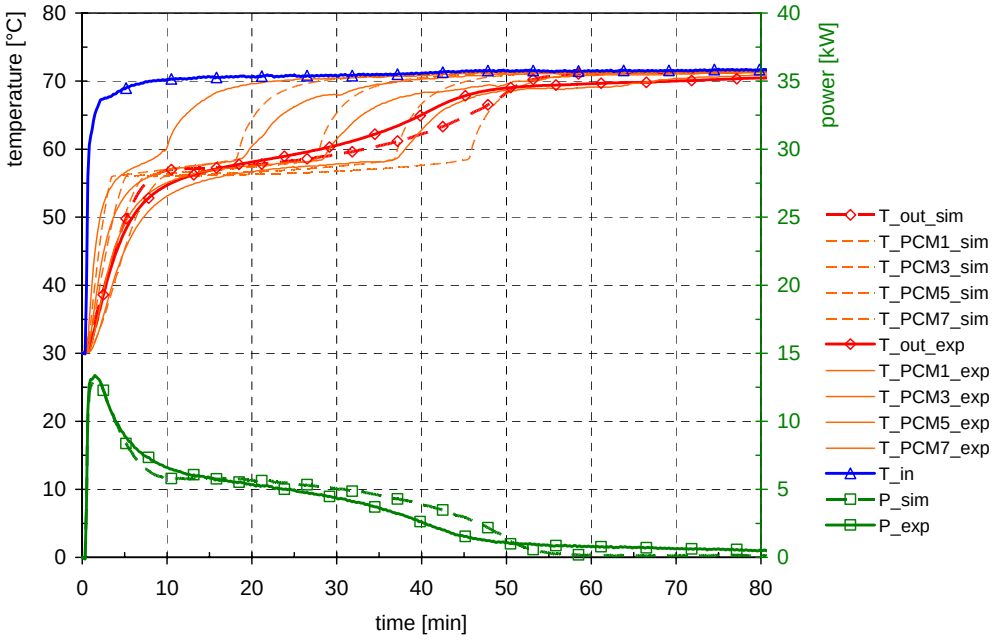

Figure 36: Comparison between simulation and measurement for charging the tank (filled with Sodium Acetate Trihydrate) with a flow rate of 370 kg/h, inlet temperature 70°C; evolution of the outlet temperature, the PCM temperatures and the charging power

Table 6: Data of the tank and the heat exchanger used in the experiments at the Institute of Thermal Engineering;, thermal properties of the used materials

masses contained in the tank		thermal properties of the used materials	
m_{PCM}	45 kg	λ_t^*	380 W/(m.K)
m_{add}	30 kg	ρ_t^*	8960 kg/m³
		$c_{p,t}^*$	0.385 kJ/(kg.K)
dimensions of the heat exchanger		λ_f^{**}	210 W/(m.K)
length tubes	0.536 mm	ρ_f^{**}	2700 kg/m³
nr. of parallel tube coils	3 -	$c_{p,f}^{**}$	0.942 kJ/(kg.K)
nr. of tubes in series	16 -	$c_{p,add}$	0.50 kJ/(kg.K)
d	11.5 mm	ρ_{PCM}	1400 kg/m³
d_w	1 mm	λ_{PCM}	0.35 W/(m.K)
		$c_{p,s,PCM}$	2.33 kJ/(kg.K)
t_l	34 mm	$c_{p,l,PCM}$	3.12 kJ/(kg.K)
t_q	34 mm	$\Delta h_{m,PCM}$	220 kJ/kg
t_f	3.3 mm	ΔT_{sc}	8 K
s_f	0.3 mm	ΔT_{hyst}	2 K

* tube material: copper

** fin material: aluminium

A comparison for a discharging process from a temperature of 70°C down to 30°C is shown in Figure 37. Here additionally the results of the modeling of the subcooling can be seen. This effect is considered in a very simple way with all nodes crystallizing at the same time, whereas there is a certain crystal growth rate in reality.

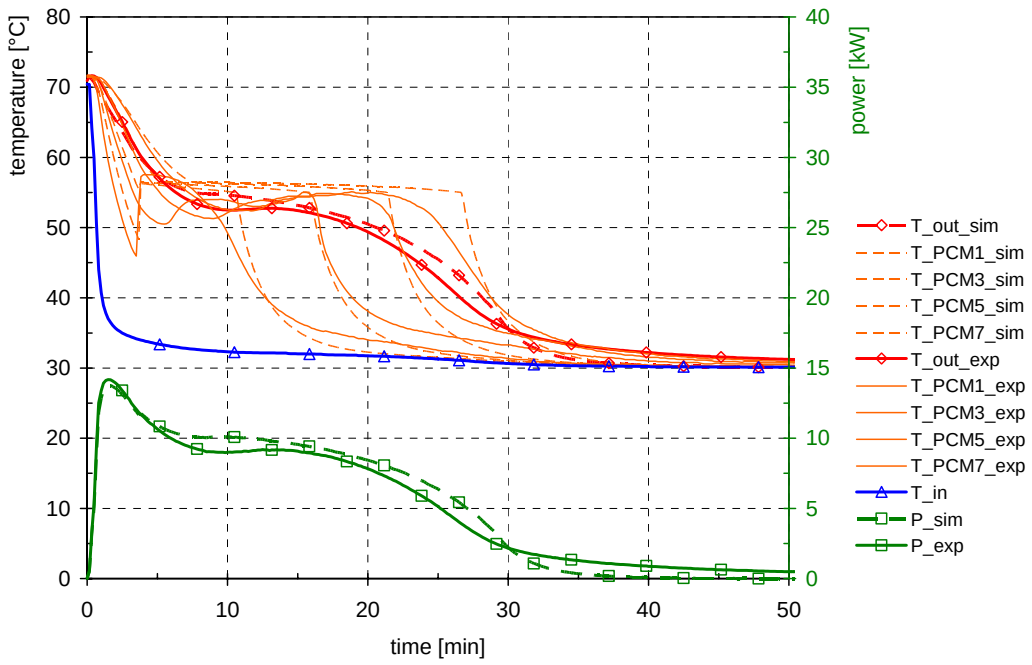

Figure 37: Comparison between simulation and measurement for discharging the tank (filled with Sodium Acetate Trihydrate) with a flow rate of 400 kg/h, inlet temperature 30°C; evolution of the outlet temperature, the PCM temperatures and the discharging power

3.8 Acknowledgements

The Austrian ministry BMVIT is thanked for the financing of the projects:

- „Fortschrittliche Wärmespeicher zur Erhöhung von solarem Deckungsgrad und Kesselnutzungsgrad sowie Emissionsverringerung durch verringertes Takten, Projekt zum IEA-SHC Task 32“ Proj. Nr. 807807
- „N-GL. IEA SHC; Task Solarthermische Anlagen mit fortschrittlicher Speicher¬technologie für Niedrigenergiegebäude“ Proj. Nr. 805790

3.9 References

Claußen T. (1993)
Entwicklung und experimentelle Verifizierung eines dynamischen Latentwärmespeichermodells; Diplomarbeit am Studiengang Diplom-Physik, Universität Oldenburg

Incropera F. P., DeWitt D. P. (2002)
Fundamentals of Heat and Mass Transfer, Fifth Edition, John Wiley & Sons, ISBN 0-471-38650-2

VDI Wärmeatlas (1997)
Wärmeübergang und Strömung in Verfahrenstechnik und Chemie, 8. Auflage, Springer Verlag

Visser H. (1986)
Energy Storage in Phase Change Materials, Development of a component model compatible with the TRNSYS transient simulation program; Department of Applied Physics, Delft University of Technology

3.10 Annex: Parameters, Inputs and Outputs of the model

List of parameters

Nr.	Name / Description	Dimension	Unit	Type
1	nr_nodes number of nodes in one heat exchanger tube [ ] the maximum number of nodes (nr_nodes * nr_tubes_ser) is 300	Dimensionless	-	integer
2	UA_loss Heat loss_rate*Surface area of the storage [W/K]	Overall Loss Coefficient	W/K	real
3	l_tubes tube length of one tube [m] (lenght of one tube through the heat exchanger, a number of several serial tubes with this length can be given with nr_tubes_ser, several parallel series of tubes can be given with nr_tubes_par)	Length	m	real
4	a_tubes arrangement of tubes: 0...aligned 1...staggered	Dimensionless	-	real
5	nr_tubes_ser number of serial tubes of length l_tube	Dimensionless	-	integer
6	nr_tubes_par number of parallel tubes of the heat exchanger [ ]	Dimensionless	-	integer
7	d outer diameter of heat exchanger pipe [mm]	Length	mm	real
8	dw wall thickness of heat exchanger pipe [mm]	Length	mm	real
9	lambda_t thermal conductivity of tube material [W/m.K]	Thermal Conductivity	W/m.K	real
10	rho_t density of the tube material [kg/m³]	Density	kg/m^3	real
11	cp_t cp of the tube material [J/kg.K]	Specific Heat	J/kg.K	real
12	tf distance between two fins + fin thickness [mm]	Length	mm	real
13	sf fin thickness [mm]	Length	mm	real
14	tl lenghtwise distance between pipes [mm]	Length	mm	real
15	tq crosswise distance between pipes [mm]	Length	mm	real
16	lambda_f thermal conductivity of the fin material [W/m.K]	Thermal Conductivity	W/m.K	real
17	cp_f cp of the fin material [J/kg.K]	Specific Heat	J/kg.K	real
18	rho_f density of the fin material [kg/m³]	Density	kg/m^3	real

19	rho_fhx density of the heat exchanger fluid [kg/m³]	Density	kg/m^3	real
20	cp_fhx cp of heat exchanger fluid [J/kg.K]	Specific Heat	J/kg.K	real
21	mass_PCM mass of PCM in the storage tank [kg] if a mass of 0 is given, then a theoretical mass will be calculated out of the heat exchanger geometry (theoretical volume) and the density of the PCM	Mass	kg	real
22	lambda_PCM thermal conductivity of storage medium [W/m.K]	Thermal Conductivity	W/m.K	real
23	rho_PCM density of storage medium [kg/m³]	Density	kg/m^3	real
24	cps_PCM cp of storage medium in the solid state [J/kg.K]	Specific Heat	J/kg.K	real
25	cpl_PCM cp of storage medium in the liquid state [J/kg.K]	Specific Heat	J/kg.K	real
26	hm_PCM latent heat of the storage medium [J/kg]	Specific Energy	J/kg	real
27	Tm1 temperature at which melting of the storage medium begins [°C]	Temperature	C	real
28	Tm2 temperature at which storage medium is fully melted [°C]	Temperature	C	real
29	dT_sc temperature difference of subcooling [K]	Temp. Difference	deltaC	real
30	dT_hyst temperature difference between melting temperature and crystallization temperature [K] often called "hysteresis", dT_hyst has to be lower or equal dT_sc !	Temp. Difference	deltaC	real
31	mass_add_cap mass of additional thermal capacity (e.g. the storage casing) [kg] the capacity will be evenly distributed over all nodes of the tank	Mass	kg	real
32	cp_add cp of additional thermal capacity [J/(kg.K)]	Specific Heat	J/kg.K	real
33	lambda_m thermal conductivity in direction m [W/(m.K)] if this parameter is set to 0, it will be calculated in the model, out of the conductivity of the fins and the PCM	Thermal Conductivity	W/m.K	real
34	lambda_n thermal conductivity in direction n [W/(m.K)] if this parameter is set to 0, it will be calculated in the model, out of the conductivity of the fins and the PCM	Thermal Conductivity	W/m.K	real
35	T_start initial temperature of the tank [°C]	Temperature	C	real
36	Pos_T1 relativ position of the first PCM temperature sensor on the heat exchanger tube	Dimensionless	-	real
37	Pos_T2	Dimensionless	-	real

	relativ position of the second PCM temperature sensor on the heat exchanger tube			
38	Pos_T3 relativ position of the third PCM temperature sensor on the heat exchanger tube	Dimensionless	-	real
39	Pos_T4 relativ position of the 4th PCM temperature sensor on the heat exchanger tube	Dimensionless	-	real

List of inputs

Nr.	Name / Description	Dimension	Unit	Type
1	T_in inlet temperature [°C]	Temperature	C	real
2	flow_in inlet flow rate [kg/hr]	Flow Rate	kg/hr	real
3	direct flow direction in the heat exchanger 1...forward (charging) 0...backward (discharging)	Dimensionless	-	integer
4	T_amb Ambient temperature of the tank [°C]	Temperature	C	real

List of outputs

Nr.	Name / Description	Dimension	Unit	Type
1	T_out Temperature at the outlet [°C]	Temperature	C	real
2	flow_out flow rate [kg/hr]	Flow Rate	kg/hr	real
3	P Power exchanged with the storage [kW]	Power	kW	real
4	T_PCM1	Temperature	C	real
5	T_PCM2	Temperature	C	real
6	T_PCM3	Temperature	C	real
7	T_PCM4	Temperature	C	real
8	Q_tot total energy of store [kWh]	Energy	kWh	real
9	P_loss Heat loss rate to ambient [kW]	Power	kW	real

4 TYPE 185 - PHASE CHANGE MATERIAL STORAGE WITH SUPERCOOLING

Jørgen M. Schultz, Department of Civil Engineering, Technical University of Denmark

4.1 General description of the principle

The supercooling characteristic of some Phase Change Materials (PCM's) can be used in seasonal PCM-storages to lower the heat loss from the storage, i.e. the storage can cool down below the melting point without solidifying and the heat of fusion energy is not released. If the supercooled storage temperature reaches the temperature of the surroundings no further heat loss will take place and the storage becomes heat loss free. When a need for energy occurs the solidification of the supercooled PCM can be activated and heat of fusion is released leading to an almost immediate rise in temperature to the melting point. Some of the heat of fusion energy is used to heat up the PCM but still a large amount of energy is available. The principle is shown in Figure 38 for Sodium Acetate Tri-hydrate that has a melting point of 58°C and a heat of fusion energy of 265 kJ/kg.

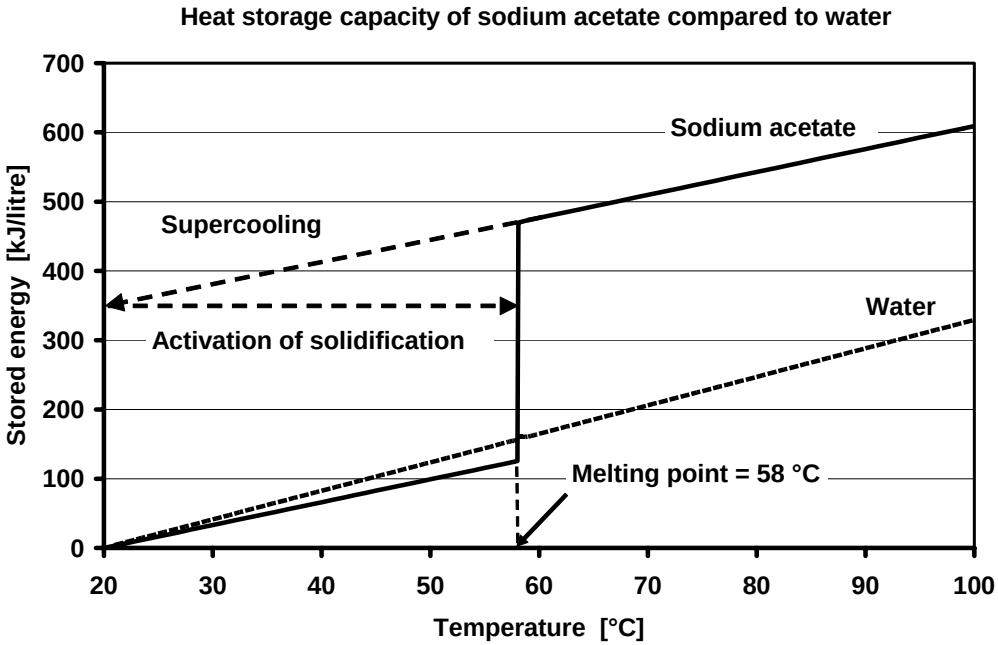

Figure 38 Illustration of energy density of sodium acetate compared to water as well as the super cooling process.

If the solidification is started the total volume will solidify, i.e. the total amount of latent heat in the supercooled PCM will be released and the supercooled state can only be reached after the total volume has been fully melted again. Therefore it is preferable to divide the total storage volume into several individual sub-volumes that can be controlled individually with respect to charging, discharging and activation of solidification, so the actual demand can be

met by activation of the required volume only. This has lead to definition of the following model.

4.2 Model description

Two different designs of the PCM storage can be modeled: 1) a cylindrical storage with the subsections stacked on top of each other (Figure 39) or 2) a distributed storage, where the sub-volumes are placed side by side e.g. for the purpose of integrating the storage in a “slab on ground” floor construction.

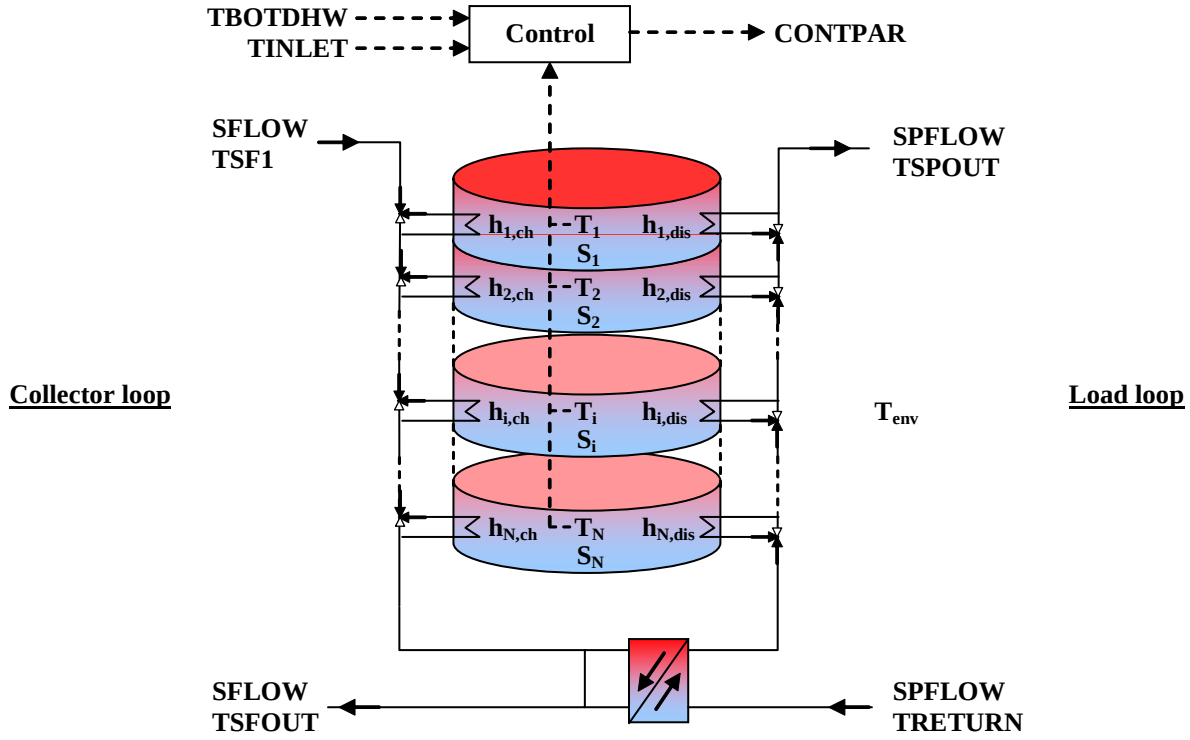

Figure 39 PCM storage divided into N subsections.

Each sub-volume includes a heat exchanger for the solar collector loop (Figure 39, left) and for the load loop (Figure 39, right). The heat transfer coefficient is assumed identical in all sub-volumes, but can be different between the solar collector loop and the load loop.

The energy content in each sub-volume is determined from the temperature, T_i, and the “degree of melting”, S_i.

The storage is uniformly insulated and heat losses to the environment takes place through all free surfaces. For the cylindrical stacked storage solution this corresponds to the surface of the cylinder.

The storage model is “an ideal model”, i.e. the boundaries between the sub-volumes are adiabatic. Furthermore, each sub-volume is treated as a lumped model with a uniform temperature and degree of melting.

The heat exchanger that connects the solar and load loop is modelled in the following way:

$$H = \frac{Heat\ transfer\ area,\ A}{\frac{1}{h_{primary}} + \frac{1}{h_{secondary}}} \quad W/K \quad , \quad h_{primary/secondary} = a \times (flow)^b$$

where, a and b are constants.

Two different charge strategies can be chosen for the model by setting the appropriate parameter:

0: the coldest sub volume is always charged first.

1: one (solidified) sub-volume is charged at the time until fully melted before charging the next

The model is developed for investigation of the benefit of supercooling, but the model can also be run without supercooling by setting the appropriate parameter:

0: no supercooling

1: with supercooling

4.3 Nomenclature

ASURF:	Surface area of PCM sub-volume [m^2]
CONTPAR:	Control parameter for controlling the collector loop pump [-]
CPCRYS:	Heat capacity of solidified PCM [J/(kg K)]
CPFLUE:	Heat capacity of liquid PCM [J/(kg K)]
CP_{fluid}:	Heat capacity of collector fluid / heat capacity of load loop fluid [J/(kg K)]
DIMENS1:	Diameter of cylindrical storage or smallest side length in rectangular storage [m]
DIMENS2:	Diameter of cylindrical storage or largest side length in rectangular storage [m]
LAYOUT:	0: Distributed sub-volumes. 1: Stacked sub-volumes
MODE1:	0: No supercooling. 1: With supercooling
MODE2:	0: Coldest sub-volume charged first. 1: One sub-volume charged at the time
NCONV1:	Number of iterations before averaging the output to the load loop
NCONV2:	Number of iterations before averaging the output to the collector loop
NFORM:	Storage cross section form: 0: Circular 1: Rectangular
NLAYER:	Number of sub-volumes
NSTEP:	Number of internal time steps **(Not used)**

QFUSION: Heat of fusion [J/kg]

QHEAT: Space heating demand [W]

QLOSS: Heat loss from PCM storage [kJ/hr]

QSTORE: Energy stored in the PCM storage [kJ/hr]

RHOCRYS: Density of solidified PCM [kg/m^3]

RHOFLUE: Density of liquid PCM [kg/m^3]

SFLOW: Mass flow in collector loop [kg/s], [kg/hr]

SPFLOW: Mass flow in load loop [kg/s], [kg/hr]

STATINIT: Initial average degree of melting in the storage [-]

STATUS: Degree of melting in PCM sub-volume [-]

STATUSMID: Average degree of melting in PCM storage [-]

TDELTA: Required difference between collector loop fluid temperature and TDHWBOT, TDHWSET and TDHWMAX to account for losses in the heat exchanger included in the model, when evaluating the charge options for the PCM storage [K]

TDHWBOT: Temperature in the bottom of the domestic hot water tank [°C]

TDHWMAX: Upper limit for domestic hot water tank temperature [°C]

TDHWSET: Set-point temperature for the domestic hot water tank [°C]

TDIFMIN: Minimum required temperature difference between collector fluid and PCM before charging if MODE2 = 1 [K]

TFUSION: PCM melting temperature [°C]

TGOAL: Required forward flow temperature in the load loop to meet the demands [°C]

TINLET: Required forward flow temperature in the space heating system [°C]

TIMESTP: Global time step in simulation [hr]

TINDOOR: Environmental temperature [°C]

TINIT: Initial average storage temperature [°C]

TOTVOL: Total storage volume [m^3]

TPCM: Temperature of PCM sub-volume [°C]

TPCMMID: Average temperature in PCM storage [°C]

TPCMOUT: Fluid temperature of solar fluid after charge of a PCM storage sub-volume [°C]

TREQ: Required forward flow fluid temperature in solar collector loop to heat exchanger if the energy demand in the load loop should be fulfilled [°C]

TRETURN Return flow temperature in space heating system [°C]

TSF: Output fluid temperature from collector [°C]

TSFOUT:	Flow temperature to collector loop [°C]
TSPIN:	Output temperature from secondary side of heat exchanger [°C]
TSPOUT:	Flow temperature to load loop [°C]
TSTEP:	Internal time step [s]
UVALUE:	Heat loss coefficient for the storage [W/(m^2 K)]
VEKAREA:	Heat transfer area in heat exchanger between the collector and the load loop [m^2]
VEKCOEF1:	Coefficient „a“ in the heat transfer calculation for the heat exchanger [-]
VEKCOEF2:	Exponent „b“ in the heat transfer calculation for the heat exchanger [-]
VOL:	Volume of PCM sub-volume [m^3]
XCH_CHAR:	Heat transfer coefficient between solar collector loop and PCM [W/K]
XCH_DISCH:	Heat transfer coefficient between load loop and PCM [W/K]
XLAMCRYS:	Thermal conductivity of solidified PCM **(Not used)** [W/(m K)]
XLAMFLUE:	Thermal conductivity of liquid PCM **(Not used)** [W/(m K)]

4.4 Mathematical description

4.4.1 Charging in case of a possible heat transfer directly from the solar collector loop to the demand loop

Based on the inputs TDHWBOT (temperature in the bottom of the DHW-tank), TINLET (required forward flow temperature in space heating loop) and QHEAT (space heating demand (>0)/(0)) and the parameter TDHWMAX (maximum allowable temperature in the DHW-tank) the required forward flow temperature (TREQ) in the solar collector loop to the heat exchanger connecting the solar and the load loop is estimated.

TSF > TREQ:

In this case there is a possibility for heat transfer to the PCM-storage and still fulfil the heating demand in the load loop.

The PCM sub-volume to be heated is determined depending on the setting of the parameter MODE2:

MODE2 = 0	**MODE2 = 1**
The model uses TREQ to choose the PCM sub-volume that, if heated by the solar fluid, cools the solar fluid to a	TSF > TFUSION: • First look for a partly melted PCM sub-volume that can be heated

temperature (TPCMOUT) that match the required forward temperature to the heat exchanger in the best possible way

sub-volume that can be heated without cooling the solar fluid to a temperature below TREQ. The partly melted sub-volume closest to be fully melted is chosen.

- If no partly melted PCM sub-volume is found the model looks for a fully crystallized sub-volume that can be heated without cooling the solar fluid to a temperature below TREQ. The crystallized sub-volume with the highest temperature is chosen.
- If no partly melted or crystallized PCM sub-volume is found the model looks for a liquid sub-volume that can be heated without cooling the solar fluid to a temperature below TREQ. The liquid sub-volume that results in the best match between TREQ and TPCMOUT is chosen.

TSF ≤ TFUSION:

- First look for a crystallized PCM sub-volume that can be heated without cooling the solar fluid to a temperature below TREQ. The crystallized sub-volume with the highest temperature, but lower than (TSF – TDIFMIN), is chosen.
- If no crystallized PCM sub-volume is found the model looks for a sub-volume that can be heated without cooling the solar fluid to a temperature below TREQ independent of the sub-volume state.

4.4.2 Charging in case of no possible heat transfer directly from the solar collector loop to the demand loop

TSF ≤ TREQ:

In this case the required temperature in the demand loop is higher than the output temperature from the collector - or there is no energy demand in the load loop.

The PCM sub-volume to be heated is determined depending on the setting of the parameter MODE2:

MODE2 = 0	**MODE2 = 1**
The model chooses the PCM sub-volume that result in the largest cooling of the fluid in the solar collector loop.	TSF > TFUSION: • First look for a partly melted PCM sub-volume that can be heated by the solar fluid. The partly melted sub-volume closest to be fully melted is

chosen.

- If no partly melted PCM sub-volume is found the model looks for a fully crystallized sub-volume that can be heated. The crystallized sub-volume with the highest temperature, but lower than (TSF – TDIFMIN), is chosen.
- If no partly melted or crystallized PCM sub-volume is found the model looks for a liquid sub-volume that can be heated the most.

TSF ≤ TFUSION:

- First look for a crystallized PCM sub-volume that can be heated. The crystallized sub-volume with the highest temperature, but lower than (TSF – TDIFMIN), is chosen.
- If no crystallized PCM sub-volume is found the model looks for a sub-volume that can be heated the most independent of the sub-volume state.

4.4.3 Heat exchange between PCM sub-volume and the fluid in the solar collector loop

Charging of a PCM sub-volume will either increase the PCM temperature or increase the degree of melting or both depending on the initial "position" on the enthalpy curve:

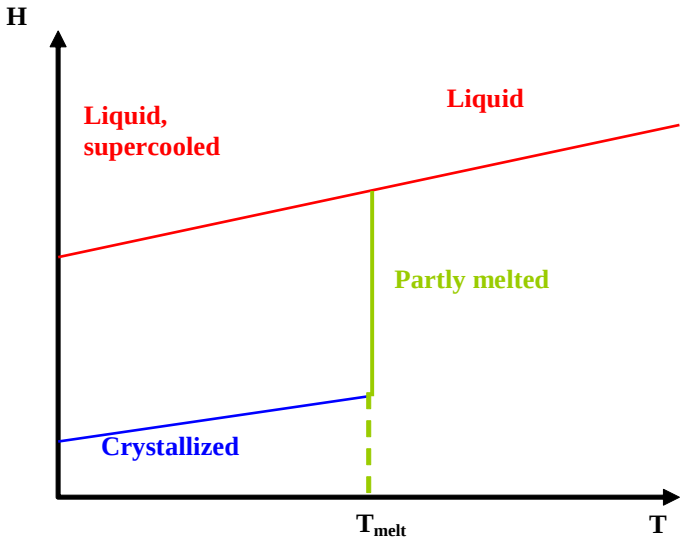

Initial state of PCM is liquid:

The PCM is liquid and energy added to the sub-volume will increase the PCM temperature described by the following equation:

$$TPCM_{new} = TSF - (TSF - TPCM_{old}) \cdot \exp\left(\frac{-TSTEP \cdot SFLOW \cdot CP_{fluid} \cdot \left(1 - \exp\left(\frac{-XCH\_CHAR}{SFLOW \cdot CP_{fluid}}\right)\right)}{VOL \cdot RHOFLUE \cdot CPFLUE} \right)$$

STATUS = 1, (degree of melting = 1)

The corresponding cooling of the solar collector loop fluid is described by:

$$TPCMOUT = TSF + \frac{VOL \cdot RHOFLUE \cdot CPFLUE \cdot (TPCM_{old} - TPCM_{new})}{SFLOW \cdot CP_{fluid} \cdot TSTEP}$$

Initial state of PCM is crystalline:

The PCM is in its crystalline form and energy added to the sub-volume will increase the PCM

$$TPCM_{new} = TSF - (TSF - TPCM_{old}) \cdot \exp\left(\frac{-TSTEP \cdot SFLOW \cdot CP_{fluid} \cdot \left(1 - \exp\left(\frac{-XCH\_CHAR}{SFLOW \cdot CP_{fluid}}\right)\right)}{VOL \cdot RHOCRYS \cdot CPCRYS} \right)$$

temperature described by the following equation:

STATUS = 0

The corresponding cooling of the solar collector loop fluid is described by:

$$TPCMOUT = TSF + \frac{VOL \cdot RHOCRYS \cdot CPCRYS \cdot (TPCM_{old} - TPCM_{new})}{SFLOW \cdot CP_{fluid} \cdot TSTEP}$$

If the calculated temperature passes the melting point, TFUSION, the PCM temperature should stay at TFUSION and the “excess” energy is used to melt some (or all) of the PCM. This is described by the following equations:

Amount of “excess” energy: $DQ = VOL \cdot RHOCRYS \cdot CPCRYS \cdot (TPCM_{new,0} - TFUSION)$

New degree of melting: $STATUS_{new,1} = STATUS_{old} + \frac{DQ}{VOL \cdot RHOCRYS \cdot QFUSION}$

Temperature in PCM sub-volume: $TPCM_{new,1} = TFUSION$

If the “excess” energy is larger than the energy needed to melt the total PCM sub-volume, $STATUS_{new,1}$ becomes larger than 1. In this case the total sub-volume has become liquid and is further heated to a higher temperature than TFUSION. This is described by the following equations:

New temperature in PCM-sub-volume: $TPCM_{new,2} = TFUSION + \frac{(STATUS_{new,1} - 1) \cdot RHOCRYS \cdot QFUSION}{RHOFLUE \cdot CPFLUE}$

New degree of melting: $STATUS_{new,2} = 1$

Initial state of PCM is partly melted:

The PCM is partly melted and energy added to the sub-volume will increase the degree of melting and if the energy added exceeds the energy to fully melt the PCM-sub-volume the PCM becomes fully liquid and the temperature will increase to above TFUSION. This is described by the following equations:

Initial cooling of solar collector loop fluid:

$$TPCMOUT = TFUSION + (TSF - TFUSION) \cdot \exp\left(\frac{-XCH\_CHAR}{SFLOW \cdot CP_{fluid}}\right)$$

Temperature in PCM sub-volume: $TPCM_{new,1} = TFUSION$

Degree of melting: $STATUS_{new,1} = STATUS_{old} + \frac{TSTEP \cdot SFLOW \cdot CP_{fluid} \cdot (TSF - TPCMOUT)}{VOL \cdot RHOCRYS \cdot QFUSION}$

The cooling of the solar collector loop fluid has to be recalculated in case the degree of melting exceeds 1:

$$TPCMOUT = TSF + \frac{VOL \cdot RHOCRYS \cdot QFUSION \cdot (STATUS_{old} - STATUS_{new,1})}{SFLOW \cdot CP_{fluid} \cdot TSTEP}$$

If the calculated degree of melting exceeds 1 it is due to the fact that the energy added to the sub-volume exceeds the energy needed to fully melt the PCM sub-volume. The “excess” energy will lead to a temperature increase in the liquid PCM. This situation is described by:

New degree of melting: $STATUS_{new,2} = 1$

New temperature in PCM-sub-volume: $TPCM_{new,2} = TFUSION + \frac{(STATUS_{new,1} - 1) \cdot RHOCRYS \cdot QFUSION}{RHOFLUE \cdot CPFLUE}$

4.4.4 Discharge of PCM-storage

Based on the inputs TDHWBOT (temperature in the bottom of the DHW-tank) and TINLET (required forward flow temperature in space heating loop) and the parameter TDHWSET (set-point temperature in the DHW-tank) the required forward flow temperature (TGOAL) in the load loop is estimated.

The PCM storage is discharged if the output temperature on the secondary side of the heat exchanger (TSPIN) is lower than TGOAL.

The PCM sub-volume to be discharged is determined in the following way:

1. First the model looks for a liquid PCM sub-volume that is able to heat the load loop fluid to the required temperature TGOAL. The sub-volume with the lowest temperature that meets the demand is chosen.
2. If no liquid sub-volume is found the model looks for a crystallized sub-volume that is able to heat the load loop fluid to the required temperature TGOAL. The sub-volume with the lowest temperature that meets the demand is chosen.
3. If neither a liquid nor a crystallized sub-volume is found the model looks for a partly melted sub-volume that is able to heat the load loop fluid to the required temperature TGOAL. The sub-volume closest to be fully crystallized that meets the demand is chosen.
4. If no liquid, crystallized or partly melted sub-volumes are found and MODE1 = 1 (supercooling possible) the model looks for a supercooled subsection, which by activation of the crystallization is able to meet the temperature demand.
5. If the temperature demand, TGOAL, cannot be met the model looks for a sub-volume that is warmer than the output temperature on the secondary side of the heat exchanger. The warmest sub-volume is chosen and the load loop fluid is preheated by the PCM storage sub-volume.

Initial state of PCM is liquid:

The PCM is liquid and discharge of the sub-volume will decrease the PCM temperature described by the following equations:

$$TPCM_{new,1} = TSPIN - (TSPIN - TPCM_{old}) \cdot \exp\left(\frac{-TSTEP \cdot SPFLOW \cdot CP_{fluid} \cdot \left(1 - \exp\left(\frac{-XCH\_DISCH}{SPFLOW \cdot CP_{fluid}}\right)\right)}{VOL \cdot RHOFLUE \cdot CPFLUE} \right)$$

$STATUS_{new,1} = 1$

The corresponding heating of the load loop fluid is described by:

$$TSPOUT = TSPIN + \frac{VOL \cdot RHOFLUE \cdot CPFLUE \cdot (TPCM_{old} - TPCM_{new,1})}{SPFLOW \cdot CP_{fluid} \cdot TSTEP}$$

In case of MODE1 = 0 (no supercooling) the temperature cannot decrease below the melting point without beginning of crystallization, so in this case the amount of discharged energy that exceeds the energy related to cooling down the PCM to the melting point comes from the heat of fusion related to the crystallization. This is described by the following equations:

New degree of melting:

$$STATUS_{new,1} = STATUS_{old} + \frac{RHOFLUE \cdot CPFLUE \cdot (TFUSION - TPCM_{new,1})}{RHOCRYS \cdot QFUSION}$$

Temperature in PCM sub-volume: $TPCM_{new,1} = TFUSION$

If $STATUS_{new,1}$ becomes negative it is due to the fact that the amount of discharged energy his larger than the heat of fusion energy + the sensible energy in the initial liquid phase of the PCM sub-volume. In this case the PCM sub-volume is fully crystallized and the PCM sub-volume temperature is further decreased:

$STATUS_{new,2} = 0$

Temperature in PCM sub-volume:

$$TPCM_{new,2} = TFUSION - \frac{RHOFLUE \cdot CPFLUE \cdot (TFUSION - TPCM_{new,1}) - RHOCRYS \cdot QFUSION}{RHOCRYS \cdot CPCRYS}$$

Initial state of PCM is crystalline:

The PCM is fully crystallized and discharge of the sub-volume will decrease the PCM temperature described by the following equations:

$$TPCM_{new,1} = TSPIN - (TSPIN - TPCM_{old}) \cdot \exp\left(\frac{-TSTEP \cdot SPFLOW \cdot CP_{fluid} \cdot \left(1 - \exp\left(\frac{-XCH\_DISCH}{SPFLOW \cdot CP_{fluid}}\right)\right)}{VOL \cdot RHOCRYS \cdot CPCRYS}\right)$$

$STATUS_{new,1} = 0$

The corresponding heating of the load loop fluid is described by:

$$TSPOUT = TSPIN + \frac{VOL \cdot RHOCRYS \cdot CPCRYS \cdot (TPCM_{old} - TPCM_{new,1})}{SPFLOW \cdot CP_{fluid} \cdot TSTEP}$$

Initial state of PCM is partly melted:

The PCM is partly melted and energy removed from the sub-volume will decrease the degree of melting and if the energy removed exceeds the energy released by fully crystallizing the PCM-sub-volume the PCM becomes fully crystallized and the temperature will decrease to below TFUSION. This is described by the following equations:

Initial heating of load loop fluid:

$$TSPOUT = TFUSION + (TSPIN - TFUSION) \cdot \exp\left(\frac{-XCH\_DISCH}{SPFLOW \cdot CP_{fluid}}\right)$$

Temperature in PCM sub-volume: $TPCM_{new,1} = TFUSION$

Degree of melting: $$STATUS_{new,1} = STATUS_{old} + \frac{TSTEP \cdot SPFLOW \cdot CP_{fluid} \cdot (TSPIN - TSPOUT)}{VOL \cdot RHOCRYS \cdot QFUSION}$$

In case the degree of melting ($STATUS_{new,1}$) becomes less than 0 it is due to the fact that the amount of discharged energy is larger than the available heat of fusion energy of the PCM sub-volume. In this case the PCM sub-volume is fully crystallized and the PCM sub-volume temperature is further decreased:

$STATUS_{new,2} = 0$

Temperature in PCM sub-volume: $$TPCM_{new,2} = TFUSION - \frac{QFUSION \cdot (0 - STATUS_{new,1})}{CPCRYS}$$

Initial state of PCM is supercooled:

The PCM is liquid and supercooled, which means that an activation of the crystallisation will make the PCM temperature increase to the melting temperature (TFUSION) and PCM will be in a partly melted state.

The degree of melting after activation of the crystallization but before discharge is lower than 1 because some of the heat of fusion energy is used to heat the PCM from its initial temperature ($TPCM_{old}$) to the melting temperature:

$$STATUS_{new,0} = 1 - \frac{RHOFLUE \cdot CPFLUE \cdot (TFUSION - TPCM_{old})}{RHOCRYS \cdot QFUSION}$$

The PCM sub-volume temperature etc. after discharge is calculated as described above in “Initial state of PCM is partly melted”

4.4.5 Method to enhance convergence

The concept of active use of supercooling introduces a discrete function - activation of a sub-volume or not, which has a large influence on the output temperatures both in the solar collector loop and the demand loop. This makes it almost impossible to make the model converge as the output temperatures may shift dramatically between iterations even if the inputs only differ slightly.

Therefore the model has a built-in convergence feature that becomes active after a user-specified number of iterations (NCONV1, NCONV2).

If the number of iterations exceeds NCONV1, the output solar collector loop fluid temperature from the model (TPCMOUT) is calculated as the successive average of the output temperature in the following iterations:

$$TPCMOUT_{average} = \frac{\sum_{i>NCONV1} TPCMOUT_i}{i - NCONV1}$$

Substitution of the actual calculated output temperature with the calculated average temperature would result in an error in the energy balance, which have to be taken into account. This is done by calculating the energy difference related to the change of the output temperature:

$$\Delta Q = SFLOW \cdot CP_{fluid} \cdot TSTEP \cdot (TPCMOUT_i - TPCMOUT_{average})$$

This energy difference is then distributed over all the sub-volumes relative to the energy content in each sub-volume. Only sub-volumes with a temperature higher than the temperature surrounding the storage (TINDOOR) are considered.

The same principle is used for the output load loop temperature from the model (TSPOUT) if the number of iterations exceeds NCONV2.

4.4.6 Calculation of heat loss

The heat loss and its influence on PCM storage temperature and degree of melting are calculated after the calculations of charging, discharging and convergence enhancement. The influence of the heat loss on PCM temperature and degree of melting is calculated for each sub-volume:

PCM liquid:

$$TPCM_{final} = TINDOOR + (TPCM_{new} - TINDOOR) \cdot \exp\left(\frac{-TSTEP \cdot ASURF \cdot UVALUE}{VOL \cdot RHOFLUE \cdot CPFLUE}\right)$$

$STATUS_{final} = 1$

PCM crystallized:

$$TPCM_{final} = TINDOOR + (TPCM_{new} - TINDOOR) \cdot \exp\left(\frac{-TSTEP \cdot ASURF \cdot UVALUE}{VOL \cdot RHOCRYS \cdot CPCRYS}\right)$$

$STATUS_{final} = 0$

PCM partly melted:

$$TPCM_{final} = TFUSION$$

$$STATUS_{final} = STATUS_{new} + \frac{TSTEP \cdot ASURF \cdot UVALUE \cdot (TFUSION - TINDOOR)}{VOL \cdot RHOCRYS \cdot QFUSION}$$

In case the heat loss leads to a change of the state, i.e. from partly to fully crystallized this is accounted for as described under "*Discharge of PCM-storage*".

4.5 TRNSYS component configuration

PARAM. NO.	LABEL	DESCRIPTION
01	TOTVOL	Total storage volume [m^3]
02	NLAYER	Number of sub-volumes
03	NFORM	Storage cross section form: 0: Circular 1: Rectangular
04	DIMENS1	Diameter of cylindrical storage or smallest side length in rectangular storage [m]
05	DIMENS2	Diameter of cylindrical storage or largest side length in rectangular storage [m]
06	LAYOUT	0: Distributed sub-volumes. 1: Stacked sub-volumes
07	UVALUE	Heat loss coefficient for the storage [W/(m^2 K)]
08	XCH_CHAR	Heat transfer coefficient between solar collector loop and PCM [W/K]
09	XCH_DISCH	Heat transfer coefficient between load loop and PCM [W/K]
10	VEKAREA	Heat transfer area in heat exchanger between the collector and the load loop [m^2]
11	VEKCOEF1	Coefficient „a“ in the heat transfer calculation for the heat exchanger [-]
12	VEKCOEF2	Exponent „b“ in the heat transfer calculation for the heat exchanger [-]
13	RHOCRYS	Density of solidified PCM [kg/m^3]
14	CPCRYS	Heat capacity of solidified PCM [J/(kg K)]
15	XLAMCRYS	Thermal conductivity of solidified PCM **(Not used)** [W/(m K)]
16	RHOFLUE	Density of liquid PCM [kg/m^3]
17	CPFLUE	Heat capacity of liquid PCM [J/(kg K)]
18	XLAMFLUE	Thermal conductivity of liquid PCM **(Not used)** [W/(m K)]
19	TFUSION	PCM melting temperature [°C]
20	QFUSION	Heat of fusion [J/kg]
21	MODE1	0: No supercooling. 1: With supercooling
22	MODE2	0: Coldest sub-volume charged first. 1: One sub-volume charged at the time
23	TDIFMIN	Minimum required temperature difference between collector fluid and PCM before charging if MODE2 = 1 [K]
24	TINIT	Initial average storage temperature [°C]
25	STATINIT	Initial average degree of melting in the storage [-]
26	TINDOOR	Environmental temperature [°C]
27	NCONV1	Number of iterations before averaging the output to the load loop
28	NCONV2	Number of iterations before averaging the output to the collector loop
29	NSTEP	Number of internal time steps **(Not used)**
30	TIMESTP	Global time step in simulation [hr]

INPUT NO.	LABEL	DESCRIPTION
01	SFLOW	Mass flow in collector loop [kg/hr]
02	TSF	Output fluid temperature from collector [°C]
03	TDHWMAX	Upper limit for domestic hot water tank temperature [°C]
04	TDHWSET	Set-point temperature for the domestic hot water tank [°C]
05	TDHWBOT	Temperature in the bottom of the domestic hot water tank [°C]
06	TINLET	Required forward flow temperature in the space heating system [°C]
07	TRETURN	Return flow temperature in space heating system [°C]
08	SPFLOW	Mass flow in load loop [kg/hr]
09	QHEAT	Required heating power in space heating loop [W]
10	TDELTA	Required difference between collector loop fluid temperature and TDHWBOT, TDHWSET and TDHWMAX to account for losses in the heat exchanger included in the model, when evaluating the charge options for the PCM storage [K]

OUTPUT NO.	LABEL	DESCRIPTION
1	TSFOUT	Flow temperature to collector loop [°C]
2	TSPOUT	Flow temperature to load loop [°C]
3	QLOSS	Heat loss from PCM storage [kJ/hr]
4	TPCMMID	Average temperature in PCM storage [°C]
5	STATUSMID	Average degree of melting in PCM storage [-]
6	QSTORE	Energy stored in the PCM storage [kJ/hr]
7	CONTPAR	Control parameter for controlling the collector loop pump [-]

4.6 Comments

The model includes a few minor theoretical errors related to the cases where the charged or discharged energy in one time step results in a shift in phase from partly melted to either fully liquid or fully crystallised. In these cases the fluid temperature is calculated from heat exchange with the PCM at its initial temperature, i.e. the melting temperature, but as illustrated below the fluid temperature should be somewhat higher or lower due to further heating or cooling of the PCM.

In case 1 in the figure below the end temperature of the PCM is higher than the melting temperature in which case the heat exchange between the fluid and the PCM at the end of the time step takes place at a lower temperature difference than at the beginning of the time step and the resulting fluid temperature in reality will be a little higher than calculated by the model. The same argument is valid for case 2 in the figure below except that the fluid in this case in reality will be a little lower than calculated.

The error is anticipated to be insignificant due to the normally small time steps used in combination with the high thermal capacity of both fluid and PCM.

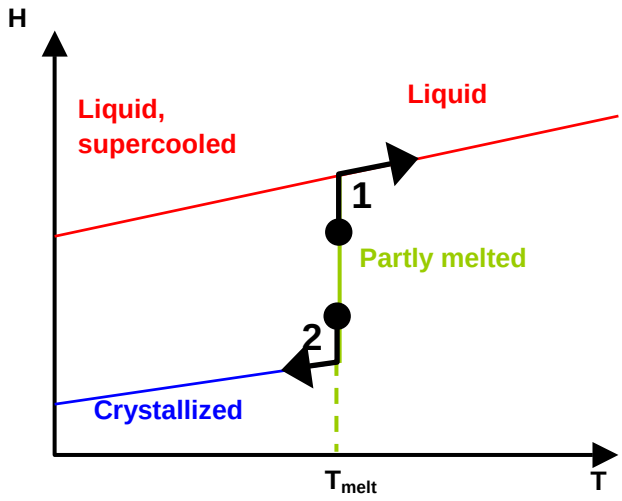

5 FINAL CONCLUSIONS

With the developed set of different PCM simulation modules by the participants of Task 32 for the TRNSYS simulation environment a powerful tool for the comparison of PCM heat stores to water stores and the optimization of hydraulic and control systems including PCM heat stores is available.

All models are validated with experimental results in the laboratories and are therefore quite reliable. Nevertheless the authors do NOT take any responsibility for the results of the models.

These tools were used to generate the results of Report C6 of IEA SHC Task 32. Of course they will be available for further research and IEA Tasks. The availability to others is handled by the respective authors.